



Climate-driven chemistry and aerosol feedbacks in CMIP6 Earth system models

Gillian Thornhill¹, William Collins¹, Dirk Olivie², Alex Archibald^{3,4}, Susanne Bauer⁵, Ramiro Checa-Garcia⁶, Stephanie Fiedler⁷, Gerd Folberth⁸, Ada Gjermundsen², Larry Horowitz⁹, Jean-Francois Lamarque¹⁰, Martine Michou¹¹, Jane Mulcahy⁸, Pierre Nabat¹¹, Vaishali Naik⁹, Fiona M. O'Connor⁸, Fabien Paulot⁹, Michael Schulz², Catherine E. Scott¹², Roland Seferian¹¹, Chris Smith¹², Toshihiko Takemura¹³, Simone Tilmes¹⁰, James Weber³,

¹Department of Meteorology, University of Reading, Reading, RG6 6BB, UK

10 ²Norwegian Meteorological Institute, Oslo, Norway

³Department of Chemistry, University of Cambridge, Cambridge, CB2 1EW, UK

⁴National Centre for Atmospheric Science, UK

⁵NASA Goddard Institute for Space Studies, 2880 Broadway

⁶IPSL/LSCE CEA-CNRS-UVSQ-UPSaclay UMR Gif sur Yvette, FRANCE

15 ⁷Max-Planck-Institute for Meteorology, Hamburg, 20146, Germany

⁸Met Office Hadley Centre, Exeter, EX1 3PB, United Kingdom

⁹GFDL/NOAA, Princeton University, Princeton, NJ 08540-6649

¹⁰National Centre for Atmospheric Research, Boulder, CO, USA

¹¹Centre National de Recherches Météorologiques, Meteo-France, Toulouse Cedex, France

20 ¹²School of Earth and Environment, University of Leeds, Leeds, LS2 9JT

¹³Research Institute for Applied Mechanics, Kyushu University, Fukuoka, Japan

Correspondence to: Bill Collins (w.collins@reading.ac.uk)

Abstract.

25 Feedbacks play a fundamental role in determining the magnitude of the response of the climate system to external forcing, such as from anthropogenic emissions. The latest generation of Earth system models include aerosol and chemistry components that interact with each other and with the biosphere. These interactions introduce a complex web of feedbacks which it is important to understand and quantify.

This paper addresses the multiple pathways for aerosol and chemical feedbacks in Earth system models. This is achieved by extending previous formalisms which include CO₂ concentrations as a state variable to a formalism which in principle includes the concentrations of all climate-active atmospheric constituents. This framework is demonstrated by applying it to the Earth system models participating in CMIP6 with a focus on the non-CO₂ reactive gases and aerosols (methane, ozone, sulphate aerosol, organic aerosol and dust).

35 We find that the overall climate feedback through chemistry and aerosols is negative in the CMIP6 Earth system models due to increased negative forcing from aerosols with warmer temperatures. Through diagnosing changes in methane emissions and lifetime we find that if Earth system models were to allow methane to vary interactively, methane positive feedbacks (principally wetland methane emissions and biogenic VOC emissions) would offset much of the aerosol feedbacks.



1 Introduction

40 Earth system models extend the complexity of climate models by representing land and ocean biospheres, atmospheric chemistry and aerosols. Within these models, natural processes, chemical reactions and biological transformations respond to changes in climate; and these processes in turn affect the climate. Therefore, the physical climate system and the biogeochemical cycles are coupled, leading to climate feedbacks that may act to further amplify or dampen the climate response to a climate forcing (Ciais et al., 2013; Heinze et al., 2019). The importance of biogeochemical feedbacks has long been
45 recognised for the longer timescales involved in paleoclimate studies, but the realisation of their relevance in the context of anthropogenic climate change is more recent. A multitude of biogeochemical feedbacks have been identified but the evaluation of their importance for future climate change remains very limited. A recent review of Earth system feedbacks (Heinze et al., 2019) examined the extensive range of feedbacks possible in an Earth system framework. Arneth et al. (2010) considered a range of terrestrial biogeochemical feedbacks interacting with the carbon cycle. O'Connor et al., (2010) reviewed potential
50 feedbacks involving methane. Carslaw et al. (2010) reviewed climate feedbacks involving natural and anthropogenic aerosols. Climate change can impact both the source strength of natural aerosols such as sea-salt, dust, biomass burning aerosols, or their precursors (dimethylsulphide (DMS), biogenic volatile organic compounds) and the lifetime of natural and anthropogenic aerosols through changes in transport and dry and wet deposition (Bellouin et al., 2011; Raes et al., 2010). Here we focus especially on those feedbacks that are mediated through changes in the abundances of reactive gases and aerosols, using data
55 from CMIP6 (Coupled Model Intercomparison Project 6) (Eyring et al., 2016) Earth system models that conducted the AerChemMIP (Aerosols and Chemistry Model Intercomparison Project) simulations (Collins et al., 2017).

Note that in this paper we use change in global mean surface temperature as our measure of climate change and for simplicity assume changes in other climate variables are proportional to this.

In section 2 we describe the theoretical framework used to diagnose the feedbacks. In section 3 we describe how the different
60 Earth System models implement the biogeochemical processes. Section 4 quantifies the feedbacks as implemented in the models. Section 5 compares these results with previous modelling and theoretical studies. Section 6 concludes. Supplementary material contains further details of the models used, and additional figures to support the process analysis of responses to dust and BVOCs.

2 Theoretical framework to analyse biogeochemical feedbacks

65 2.1 Theory

In order to compare climate feedbacks we need to compare them on a common scale of the change in the top of atmosphere radiation balance following a unit warming (in $\text{W m}^{-2} \text{K}^{-1}$) (e.g. Gregory et al., 2009). Following Gregory et al. (2004) the radiative imbalance ΔN from an imposed forcing ΔF is given by $\Delta N = \Delta F + \alpha \Delta T$ where ΔT is the global mean change in surface temperature and α is the climate feedback parameter ($= \frac{d\Delta N}{d\Delta T}$). The total derivative $\frac{d\Delta N}{d\Delta T}$ can be split into a set of partial



70 derivatives $\frac{d\Delta N}{d\Delta T} = \sum_i \frac{\partial \Delta N}{\partial \Delta C_i} \frac{\partial \Delta C_i}{\partial \Delta T} = \sum_i \alpha_i$, where the α_i are the individual feedback terms due to a change in a climate variable
 C_i . For feedbacks involving changes in composition, the ΔC_i can represent changes in reactive gas or aerosol burdens or
emissions. $\alpha_i = \frac{\partial \Delta N}{\partial \Delta C_i} \frac{\partial \Delta C_i}{\partial \Delta T}$ can then be expressed as $\phi_i \gamma_i$, where ϕ_i is the radiative efficiency of the species per burden (Wm^{-2}
 Tg^{-1}) or per emission ($\text{Wm}^{-2} (\text{Tg yr}^{-1})^{-1}$), and γ_i is the change in species burden or emission with climate (Tg K^{-1} or $\text{Tg yr}^{-1} \text{K}^{-1}$).
75 The radiative efficiencies are based on effective radiative forcing (ERF) (Myhre et al., 2013) to include rapid adjustments to
changes in composition.

2.2 Applying the theory to Earth system models

With Earth system models, the ϕ_i and γ_i coefficients can be diagnosed from idealised simulations in which only climate or
composition are changed. Here we use the set of simulations specified under the CMIP6 project (Eyring et al., 2016).

80 The γ_i are diagnosed from a pair of idealised climate change scenarios, *piControl* where composition is maintained at a level
representative of 1850 conditions, and *abrupt-4xCO2* where CO_2 concentrations are abruptly quadrupled, but no other species
are directly perturbed. We take the 30-year time means from years 121-150 of these simulations for both the surface
temperature change and the burden/emission changes. The global mean surface temperature changes are therefore not the same
as the equilibrium climate sensitivities (ECSs) derived from the *abrupt-4xCO2* but are temperatures consistent with the
averaging period for the burden or emissions. The γ_i are calculated from the change in emission or burden divided by the
85 temperature change.

The ϕ_i coefficients for changes in emissions are derived from pairs of AerChemMIP simulations, *piClim-control* where
composition and climate are maintained at a level representative of 1850 conditions, and experiments *piClim-2x* (table 1) in
which individual natural emission fluxes are doubled. The climate change in these simulations is restricted by using fixed sea
surface temperatures and sea ice cover (Collins et al., 2017) for a 30-year mean of the *piControl* simulation. The ERFs are
90 determined by the mean difference in top of atmosphere radiative fluxes between the *piClim-2x* and the *piClim-control* over a
30-year period. The ϕ_i are calculated from the ERF divided by either the change in emission or change in burden, depending
on the units of γ_i above.



Experiment	Flux to be doubled
<i>piClim-control</i>	None
<i>piClim-2xdust</i>	Dust
<i>piClim-2xss</i>	Sea salt
<i>piClim-2xDMS</i>	Oceanic DMS
<i>piClim-2xNOx</i>	Lightning NO _x
<i>piClim-2xVOC</i>	Biogenic VOCs

95 **Table 1: List of simulations for diagnosing ERFs of natural emitted species. The specified natural emission fluxes are doubled compared to the 1850 control.**

For ϕ_{O_3} a radiative efficiency of 0.042 W m^{-2} per Dobson Unit (DU) is used in the troposphere (Stevenson et al., 2013).

The ESM setups here, even with tropospheric chemistry, still constrain methane to specified concentrations at the surface. This means that any feedbacks mediated through changes in oxidising capacity have a negligible effect on methane. It is however possible to diagnose the change in methane that would be expected, if it were not constrained, from the change in its lifetime

100 $\frac{\Delta C}{C} = \left(\frac{\Delta\tau}{\tau} + 1\right)^f - 1 \approx f \frac{\Delta\tau}{\tau}$, where C is the methane concentration, τ is the total methane lifetime (including loss to soils) and f is the feedback of methane on its own lifetime (Fiore et al., 2009). The radiative forcing from the change in concentration is calculated using the formula from Etminan et al., (2016) scaled by 1.65 to account for change in ozone and stratospheric water vapour (Myhre et al., 2013). This gives 1.15 W m^{-2} per fractional change in methane lifetime (based on 1850 baseline concentrations of methane and N₂O). Changes in methane concentration due to changes in emissions ΔE are given by $\Delta C =$
105 $\Delta E \tau f \left(\frac{m_{\text{air}}}{m_{\text{CH}_4}}\right) / M_{\text{atm}}$, where $\tau=9.25$ years, and $f=1.34$ (Myhre et al., 2013). m_{air} and m_{CH_4} are the relative molecular masses of air and methane.

3 Model descriptions

3.1 Model implementation of aerosols, tropospheric and stratospheric chemistry

We use results from 6 Earth system models that contributed simulations under the AerChemMIP *piClim-2x* experimental setup.

110 All six models have interactive aerosol schemes, four have interactive stratospheric chemistry and three have interactive tropospheric chemistry. The level of sophistication of the chemistry can affect the modelled responses to the emissions of reactive gases. For instance, in models without interactive tropospheric chemistry changes in biogenic volatile organic compound emissions (BVOCs) affect only organic aerosols, whereas in models with interactive tropospheric chemistry they also affect ozone, methane lifetime, and potentially the oxidation of other aerosol precursors.

115



	Tropospheric chemistry	Stratospheric chemistry	Reference
NorESM2	No	No	(Olivié et al., in prep; Kirkevåg et al., 2018))
UKESM1	Interactive	Interactive	(Archibald et al., 2019; Sellar et al., 2019)
CNRM-ESM2	No	Interactive	(Séférian et al., 2019)
MIROC6	No	No	(Tatebe et al., 2019)
GFDL-ESM4	Interactive	Interactive	(Horowitz et al., in prep)
CESM2-WACCM	Interactive	Interactive	(Gettelman et al., 2019)

Table 2 Sophistication of gas-phase chemistry used in the Earth system models (For further details see (Thornhill et al., submitted) .

3.2 Model implementation of natural emissions

3.2.1 Land

The principle land-based natural emissions are dust and BVOCs (table 3).

- 120 Dust emissions are parameterised as a function of surface wind speeds or wind stress, and account for the amount of bare soil, soil type, and aridity (Ackerley et al., 2012; Collins et al., 2011; Evan et al., 2014; Fiedler et al., 2016; Huneus et al., 2011; Shao et al., 2011; Zender et al., 2004). There is a variation between the models in the sizes considered, whether binned or modal, and the optical properties of the dust particles (Kok et al., 2018; Xie et al., 2018). Table S1 lists the parameterizations for desert-dust aerosol for the contributing models and the simulated dust-aerosol sizes.
- 125 BVOC emissions are parametrised as a function of vegetation type and cover, and also temperature and photosynthesis rates (gross primary productivity) (Guenther, 1995; Pacifico et al., 2011; Sporre et al., 2019; Unger, 2014). Some parameterisations also include dependence on CO₂ concentrations (Pacifico et al., 2012). Models differ in the speciation of the VOCs emitted but typically include isoprene and monoterpenes, with different emission parameterisations for different species. The ability of VOCs to form secondary organic aerosol are typically parameterised as a fixed yield (Mulcahy et al., 2019). For further
- 130 details see table S1 and references therein.



	Dust	VOC
NorESM2	LAI varies	Dependence on PAR, temperature
UKESM1	Interactive vegetation	Dependence on PAR, temperature, vegetation
CNRM-ESM2	Prescribed land cover	Prescribed
MIROC6	LAI varies	Prescribed
GFDL-ESM4	Interactive vegetation	Dependence on PAR, temperature. Not dependent on vegetation.
CESM2-WACCM	LAI varies	Dependence on PAR, temperature

Table 3 Levels of complexity of vegetation included in the land-based emissions schemes of dust and BVOCs for the ESMs.

3.2.2 Marine

The principle ocean emissions are of sea salt, dimethyl-sulphide (DMS) and primary organic aerosols (table 4).

135 The air-sea exchange processes for these emissions are parameterised as a function of wind speed and sometimes temperature (Gong, 2003; Jaeglé et al., 2011).

Changes in DMS emissions can be initiated by various factors such as changes in temperature, insolation, depth of the ocean-mixed layer, sea-ice extent, wind strength, nutrient recycling, or shift in marine ecosystems (Heinze et al., 2019). The surface sea water concentrations of DMS are prescribed in some models (CNRM-ESM2, GFDL-ESM4, MIROC6, CESM2-WACCM) and calculated interactively from ocean biogeochemistry in others (UKESM1, NorESM2). Oceanic organic aerosol emissions are also wind-speed dependent and in addition depend on chlorophyll concentrations generated either from interactive biogeochemistry or observation-based chlorophyll concentrations in models without ocean biogeochemistry components.

140



	Sea salt	DMS	Oceanic organic aerosol
NorESM2-LM	Temperature and wind dependent	Interactive biogeochemistry for sea water DMS concentration, wind speed and temperature for air-sea DMS flux	Interactive biogeochemistry for Chlorophyll concentrations; wind speed; sea salt emission flux
UKESM1	Wind speed	Interactive biogeochemistry	Interactive biogeochemistry
CNRM-ESM2-1	Temperature, wind speed	Prescribed emissions	
MIROC6	Wind speed	Dependent on wind speed and chlorophyll	Dependent on wind speed and chlorophyll
GFDL-ESM4	Temperature, wind speed	Wind speed. Prescribed sea water concentration	
CESM2-WACCM	Wind speed	Wind speed. Prescribed sea water concentration	Wind speed

Table 4 Levels of complexity of marine emissions in the ESMs

145 3.2.3 Lightning

The models with tropospheric chemistry (UKESM1, GFDL-ESM4, CESM2-WACCM) all include parameterisations of the emission of nitrogen oxides (NO_x) from lightning, related to the height of the convective cloud top (Price et al., 1997; Price and Rind, 1992). The lightning frequency depends strongly on the convective cloud top height, and the ratio of cloud-to-cloud versus cloud-to-ground lightning depends on the cold cloud thickness (from 0°C to the cloud top).

150 4 Quantification of feedbacks

The feedbacks in this section are all derived from the difference between the *piControl* and *abrupt-4xCO2* CMIP6 experiments. The Earth system models all respond with different levels of climate change, so all climate feedbacks are normalised to the change in global mean surface temperature between *abrupt-4xCO2* and *piControl* for the 30-year period years 121-150 (table 5). There is a factor of nearly two between the temperature responses of the models. Since this timeframe is not long enough
 155 for the models to have reached equilibrium these temperatures are not the same as equilibrium climate sensitivity (ECS).



	CNRM-ESM2	UKESM1	MIROC6	NorESM2	CESM2-WACCM	GFDL-ESM4
ΔT_{4xCO_2} (K)	6.02	7.46	4.01	3.96	6.37	3.93

Table 5: Change in global mean surface temperature following an abrupt quadrupling of CO₂ concentrations. Difference between *abrupt-4xCO₂* and *piControl* averaged over the years 121-150.

4.1 Aerosol species

160 4.1.1 Desert Dust

The *2xdust* perturbation is applied by scaling the parameterisation in the emission scheme. Since changing dust emissions will affect the boundary layer meteorology the net effect is not an exact doubling of the emissions (table 6). Four of the five models in AerChemMIP have a negative radiative forcing for doubled dust aerosols as the negative shortwave radiative effects outweigh the positive longwave radiative effects of dust aerosols (figures 1(a), S1(a-e); table 6). The only exception is CNRM-ESM2, where the global shortwave forcing is also positive, explaining the different sign of the ERF compared to the other models. The ERF for GFDL-ESM4 is not significantly different from zero. UKESM1 has by far the largest dust emissions (and change from doubling) because it includes particles that are emitted and deposited in the same timestep. CNRM-ESM2 also includes large particles (up to 50 μ m). These models however have similar changes in dust aerosol optical depth (AOD) compared to the other models and hence the magnitude of the forcing efficiency per change in AOD is not out of line with the others. MIROC6 has the strongest forcing even with the lowest emissions and smallest change in AOD, thus giving it the largest forcing efficiency per AOD (figure S1 (f-j)).

The response of dust aerosols to *abrupt-4xCO₂* (figure 1(b)) is substantially different across the model ensemble. Three models (CNRM-ESM2, MIROC6 and GFDL-ESM4) show an increase in dust emission in a *4xCO₂* climate due to increased aridity and near-surface wind speeds, whereas UKESM has a decrease in dust emissions with more CO₂ due to increased fertilisation of the vegetation (hence less bare soil) paired with decreased near-surface winds. NorESM2 shows near zero change. The spatial pattern of the opposing response of dust emission to *4xCO₂* in the two most extreme models, UKESM1 and CNRM-ESM2, is consistent with the responses in 10m-wind speed to *4xCO₂* (figure S2). These clearly reflect larger (smaller) increases in mean winds over regions where the mean emission amount is larger (smaller) for *4xCO₂* compared to the pre-industrial climatology. The increase or decrease in winds is also likely to be affected by changes in vegetation in semi-arid regions, e.g., the Sahel.

As well as affecting the emissions, changing climate can also affect the removal of dust. In all models except UKESM1 the lifetime of dust increases. The effect of an increase in lifetime can be seen by comparing the change in AOD. The modelled changes in dust AOD in the *abrupt-4xCO₂* experiment are one and a half to twice as large (for those models where lifetime increases) as would be expected assuming a linear scaling with emissions across all size ranges (“scaled AOD” in table 6).



185 The climate feedback parameter for dust is given by the product of the radiative efficiencies (ϕ) with the sensitivities to climate
(γ). These vary from -0.016 to $+0.048 \text{ W m}^{-2} \text{ K}^{-1}$ with a multi-model mean of $-0.003 \pm 0.008 \text{ W m}^{-2} \text{ K}^{-1}$, i.e. averaging to a value
near zero. Although some models obtain similar feedback terms, this is not necessarily for the same reason. For instance,
CNRM-ESM2 and UKESM1 have a positive dust feedback, though for opposite reasons; an increase in positive forcing in
CNRM-ESM2 and a decrease in negative forcing in UKESM1. For instance, NorESM2 has a large ERF for doubled dust
190 emissions, the small change in dust emission for $4xCO_2$, however, does not lead to a large feedback for that model.

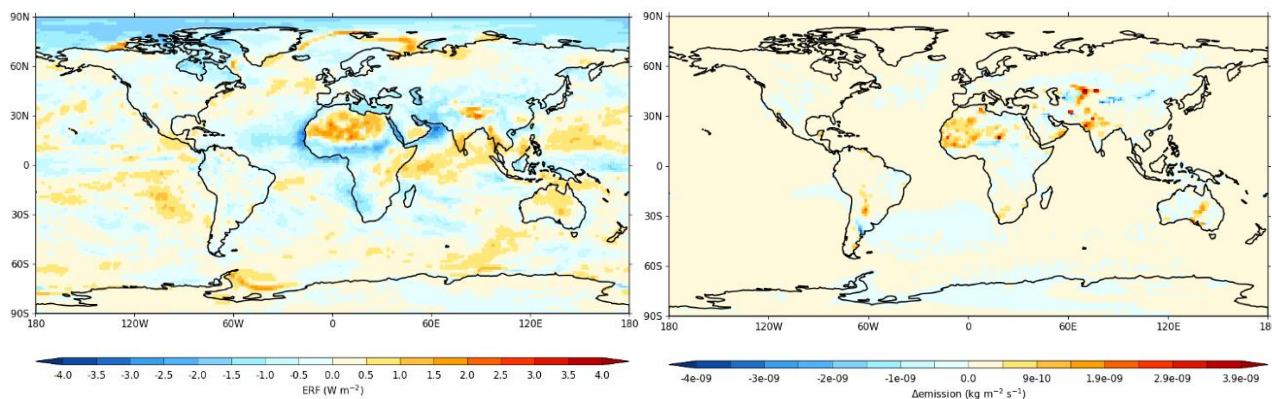


Figure 1 Multi-model mean (a) ERF from *piClim-2xdust* vs *piClim-control*, (b) Change in dust emissions for *abrupt-4xCO2* vs *piControl*.



	CNRM-ESM2	UKESM1	MIROC6	NorESM2	GFDL-ESM4	Multi-model
Emission control Tg yr ⁻¹	2750	8066	1106	1661	1981	
ΔEmission 2xdust Tg yr ⁻¹	2877	8256	1065	1397	1989	
ERF 2xdust W m ⁻²	0.09±0.03	-0.07±0.03	-0.18±0.04	-0.14±0.07	-0.00±0.03	
ERF/ Emission W m ⁻² (Tg yr ⁻¹) ⁻¹	3.1±1.0E-5	-8.9±3.6E-6	-1.7±0.4E-4	-1.1±0.5E-4	-0.2±1.5E-5	
ERF/AOD W m ⁻²	8.0±2.7	-5.8±2.4	-25.6±5.6	-6.0±2.8	-0.2±1.6	
ΔEmission/ΔT Tg yr ⁻¹ K ⁻¹	65±4	-109±15	70.±7	-9±0	181±10	
Δlifetime/ΔT % K ⁻¹	2.6±0.2	-0.4±0.4	1.9±0.9	1.2±0.3	3.7±0.6	
scaled AOD/ΔT K ⁻¹	2.5±0.2E-4	-1.7±0.2E-4	4.8±0.4E-4	-1.6±E-4	17.3±1.0E-4	
4xCO ₂ ΔAOD/ΔT K ⁻¹	6.0±0.3E-4	-2.6±0.6E-4	6.3±0.5E-4		26.5±1.3E-4	
α emissions W m ⁻² K ⁻¹	0.0020±0.0007	0.0010±0.0004	-0.012±0.003	0.0010±0.0005	-0.0004±0.0027	-0.002±0.005
α AOD W m ⁻² K ⁻¹	0.0048±0.0016	0.0015±0.0007	-0.016±0.004		-0.0006±0.0042	-0.003±0.008

195 **Table 6. Dust radiative efficiencies by emission and AOD from 2xdust experiments. Changes in emission and AOD from abrupt-4xCO₂. “scaled” refers to scaling the 2xdust relations between AOD and emissions by the 4xCO₂ changes in emissions. alpha values are calculated assuming ERF is proportional to emissions or AOD. Uncertainties for each model are errors in the mean based on interannual variability. Uncertainties in the multi-model results are standard deviation across the models.**

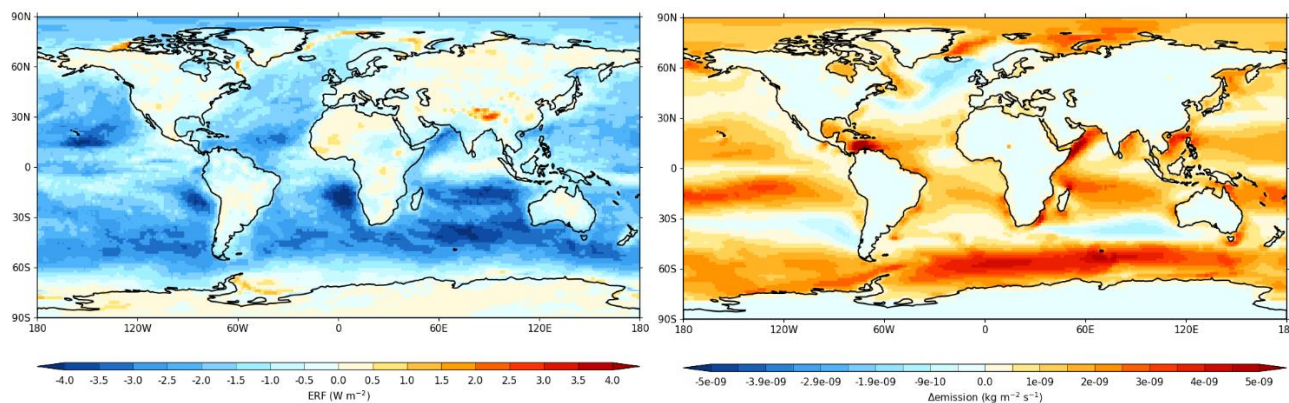
4.1.2 Sea Salt

200 All models show a strong negative forcing to double sea salt emissions (figure 2(a), table 7), although the ERF for MIROC6 is significantly smaller than the others. The emissions and mass loading for the CNRM-ESM2 model are approximately twenty times those of the other models, although the AOD change is similar to other models. All models show a similar forcing efficiency per AOD change. All models show an increase in sea salt emissions in the Southern Ocean in 4xCO₂ (figure 2(b)) due to increased wind speeds, with a general tendency for decreases elsewhere due to rising temperatures (Jaeglé et al., 2011).

205 The global mean change in emissions is positive in all models except MIROC6. For models showing an increased lifetime in 4xCO₂ the modelled increase in AOD is larger than that expected from scaling the emissions change. Although emissions (and



the mass burden) of sea salt decrease in MIROC6 the AOD increases. The mean feedback is $-0.031 \pm 0.31 \text{ W m}^{-2} \text{ K}^{-1}$ based on emissions, and $-0.060 \pm 0.56 \text{ W m}^{-2} \text{ K}^{-1}$ based on the increase in AOD. The signs are consistently negative except for the emission-based feedback for MIROC6.



210

Figure 2 Multi-model mean (a) ERF from *piClim-2xss* vs *piClim-control*, (b) Change in sea-salt emissions for *abrupt-4xCO2* vs *piControl*.



	CNRM-ESM2	UKESM1	MIROC6	NorESM2	GFDL-ESM4	Multi-model
Δ Emission $2x_{SS}$ Tg yr ⁻¹	64939	5500	3577	3771	5675	
ERF $2x_{SS}$ W m ⁻²	-1.04±0.03	-1.29±0.03	-0.35±0.04	-2.28±0.07	-1.84±0.03	
ERF/ Emission W m ⁻² (Tg yr ⁻¹) ⁻¹	-1.61±0.04 E-5	-2.30±0.05E-4	-9.72±1.12E-5	-6.0±0.2E-4	-3.20±0.07 E-4	
ERF/AOD W m ⁻²	-19.8±0.6		-25±3	-26±0.8	-38.7±0.8	
Δ Emission/ Δ T Tg yr ⁻¹ K ⁻¹	2570±87	6.0±2.6	-3.93±2.6	72±4	258±9	
Δ lifetime/ Δ T % K ⁻¹	0.44±0.13	-0.20±0.06	-0.68±0.09	-0.92±0.14	1.8±0.2	
Scaled AOD/ Δ T K ⁻¹	20.8±0.7E-4		-0.16±0.10E-4	17±1E-4	21.6±0.8E-4	
$4xCO_2$ Δ AOD/ Δ T K ⁻¹	24.8±0.8E-4		0.62±0.20E-4		33.6±1.0E-4	
α emissions W m ⁻² K ⁻¹	-0.041±0.002	-0.0014±0.0006	0.0004±0.0003	-0.044±0.003	-0.084±0.004	-0.031±0.031
α AOD W m ⁻² K ⁻¹	-0.049±0.002		-0.0015±0.0005		-0.130±0.005	-0.060±0.053

215 **Table 7. Radiative efficiencies by emission and AOD from $2x_{SS}$ (sea-salt). Changes in emission and AOD from $4xCO_2$. “scaled” refers to scaling the $2x_{SS}$ relations between AOD to emissions by the $4xCO_2$ changes in emissions. α values are calculated assuming ERF is proportional to emissions or AOD. Uncertainties for each model are errors in the mean based on interannual variability. Uncertainties in the multi-model results are standard deviation across the models. Not all models provided AOD diagnostics.**

4.1.3 DMS

220 All models except CNRM-ESM2 have interactive DMS emissions that vary with climate (wind speed), and two also include interactive ocean biogeochemistry (UKESM1 and NorESM2). The latter two performed the $2xDMS$ experiment. CNRM-ESM2 also ran the $2xDMS$ experiment but uses prescribed emissions that are independent of climate. The ERF for $2xDMS$ is negative for all three models that ran this experiment (figure 3(a)), though less strongly so for CNRM-ESM2. Three of the models with interactive emissions show a decrease in sulphur emissions in $4xCO_2$ where the tropical decrease more than compensates for the increase along the edge of the sea ice retreat. GFDL-ESM4 shows an increase in overall sulphur emissions.

225 The multi-model mean is shown in figure 3(b). Since not all data is available for all models, we use the multi-model radiative efficiencies (by emission and by mass) and the multi-model sensitivities (of emissions and mass) to climate in order to calculate the multi-model feedback (table 8). The strong positive DMS increase in GFDL-ESM4 weakens the multi-model mean decrease in emission with climate. The multi-model mean emission-based α is therefore near-zero (within the uncertainty



range). There is an increased sulphur mass in all models in the $4xCO_2$ simulation due to an increase in the sulphate lifetime.
230 When scaled by the radiative efficiency for DMS emissions (which might not be appropriate for a lifetime increase) this leads to negative α ($-0.048 \pm 0.028 \text{ W m}^{-2} \text{ K}^{-1}$).

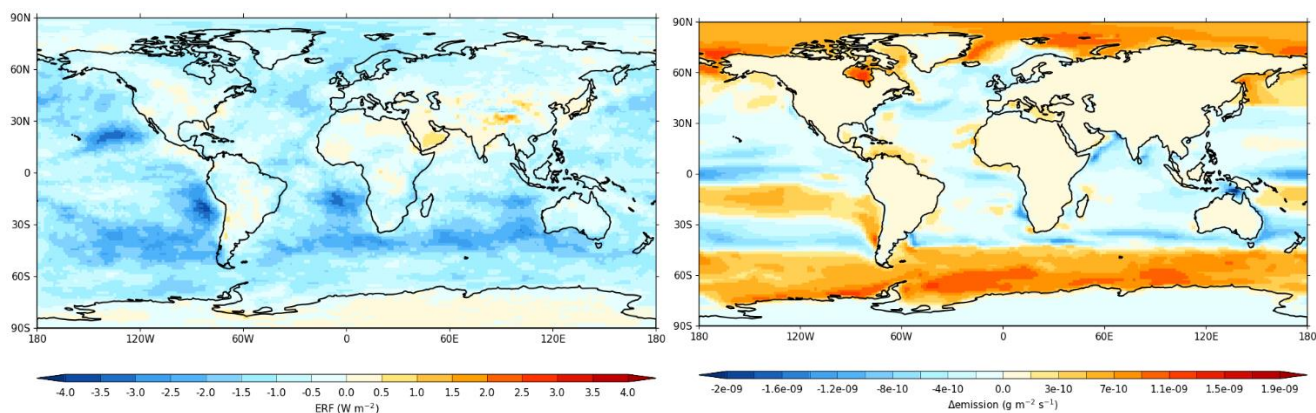


Figure 3 Multi-model mean (a) ERF from *piClim-2xDMS* vs *piClim-control*, (b) Change in DMS emissions for *abrupt-4xCO2* vs *piControl*



	CNRM-ESM2	UKESM1	MIROC6	NorESM2	GFDL-ESM4	Multi-model
ERF $2x$ DMS W m ⁻²	-0.37±0.03	-1.22±0.03		-1.27±0.07		
ERF/ Emission W m ⁻² (Tg(S) yr ⁻¹) ⁻¹	-0.0089±0.0007	-0.0386±0.0010		-0.0348±0.0019		-0.027±0.013
ERF/mass W m ⁻²	-3.8±0.3	-3.15±0.08		-5.4±0.3		-4.1±1.0
ΔEmission/ΔT Tg(S) yr ⁻¹ K ⁻¹		-0.07±0.02	-0.014±0.004	-0.36±0.03	0.39±0.03	-0.01±0.24
Scaled mass/ΔT Tg(S) K ⁻¹		-8.9±2.1E-4		-23±2E-4		
$4x$ CO ₂ Δmass/ΔT Tg(S) K ⁻¹	25.4±0.9E-4	186±7E-4	59±2E-4	14±6E-4	172±7E-4	120±6E-4
Δlifetime/ΔT % K ⁻¹	1.98±0.4	2.48±0.06	1.91±0.07	2.73±0.11	2.42±0.09	
α emissions W m ⁻² K ⁻¹		0.0028±0.0007		0.0125±0.0013		0.000±0.007
α mass W m ⁻² K ⁻¹	-0.0097±0.0009	-0.059±0.003		-0.075±0.005		-0.048±0.028

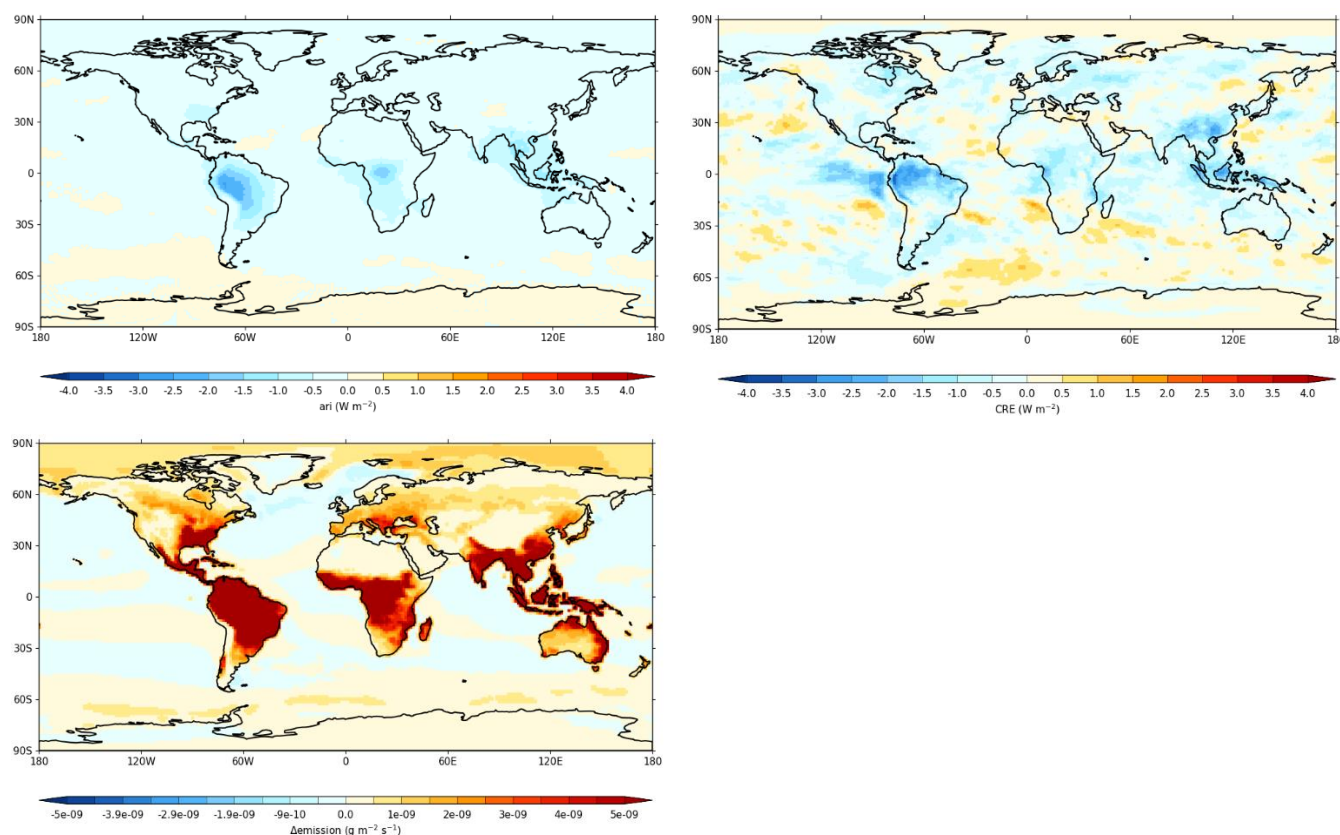
235 **Table 8. Radiative efficiencies by emission and mass from $2x$ DMS. Changes in emission and mass from $4x$ CO₂ experiment. Emissions**
 are for DMS or SO₂+SO₄ depending on the model. “scaled” refers to scaling the $2x$ DMS relations between mass and emissions by
 240 the $4x$ CO₂ changes in emissions. α values are calculated assuming ERF is proportional to emissions or mass. Multi-model mean
 values of α use the multi-model mean radiative efficiencies and sensitivities to climate, rather than being an average of the individual
 model α values. Uncertainties for each model are errors in the mean based on interannual variability. Uncertainties in the multi-
 model results are standard deviation across the models. MIROC6 and GFDL-ESM4 did not perform the $2x$ DMS experiment, but
 DMS changes are diagnosed from their $4x$ CO₂ experiments. DMS emissions do not vary in the CNRM-ESM2 $4x$ CO₂ experiment.

4.1.4 Organic aerosol

Biogenic VOC emissions lead to both organic aerosol and ozone production (in those models with tropospheric chemistry). It
 is therefore difficult to distinguish the two in the ERFs in these models. An estimate of the direct aerosol effect can be
 245 determined by additional radiation diagnostics that are run without the contribution of aerosols “aerosol-free” (ERF_{af}), for clear
 sky conditions (ERF_{cs}), and both clear sky and aerosol free (ERF_{csaf}) (Ghan, 2013). Here the aerosol direct effect is ERF-ERF_{af}
 and the cloud effect is ERF_{af}-ERF_{csaf} (although this may include cloud forcing due to adjustments caused by the ozone changes
 too). The direct aerosol and cloud radiative effects are shown in figure 4. These estimated aerosol forcing changes are
 significant (between -0.3 and -0.69 W m⁻²). The most negative forcing comes from the NorESM2 model which has no changes
 250 in gas-phase chemistry (table 9).



In terms of aerosol, there is an increase in organic aerosol (OA) mass and expected increase in AOD with very similar spatial pattern when the emission of BVOCs is doubled. Changes to cloud droplet number concentration are more complex and may not be spatially co-located with the changes to BVOC emission (figure S4). Whilst the additional secondary organic aerosol can grow particles to a size where they can act as cloud condensation nuclei, this process can also enhance the aging rate of particles removing them from the atmosphere more quickly. In addition, for models with interactive tropospheric chemistry, the decrease in oxidant concentrations resulting from a doubling of VOC emissions can prevent the oxidation of sulphur containing species that might otherwise have formed aerosols, leading to a reduction in CDNC. In the $4xCO_2$ experiments, these models also simulate an increase in primary organic aerosol emission from the ocean which adds to the OA mass on top of the effect of BVOC emissions. The feedback factors are negative and very strong in some models, ranging from -0.003 to $-0.276 \text{ W m}^{-2} \text{ K}^{-1}$ based on emissions and -0.025 to $-0.359 \text{ W m}^{-2} \text{ K}^{-1}$ based on mass assuming all OA has the same radiative efficiency as that from vegetation.



265 **Figure 4** Multi-model mean (a) Aerosol direct effect from *piClim-2xVOC* vs *piClim-control*, (b) cloud radiative effect from *piClim-2xVOC* vs *piClim-control*, (c) Change in organic aerosol emissions for *abrupt-4xCO2* vs *piControl*.



	UKESM1		NorESM2		GFDL-ESM4		CESM2- WACCM	Multi-model
ERF $2xVOC$ $W m^{-2}$	direct	cloud	direct	cloud	direct	cloud	-0.31	
	-0.19 ± 0.03	0.12 ± 0.03	-0.18 ± 0.07	-0.55 ± 0.07	-0.21 ± 0.04	-0.30 ± 0.04		
ERF/ Emission $W m^{-2} (Tg) yr^{-1})^{-1}$	$-1.0 \pm 0.4E-4$		$-11.8 \pm 1.2E-4$		$-10.9 \pm 0.6E-4$		$-4.7 \pm 0.6E-4$	$-7 \pm 4E-4$
ERF/mass $W m^{-2}$	-0.19 ± 0.08		-0.56 ± 0.06		-0.70 ± 0.04		-0.29 ± 0.04	-0.34 ± 0.16
Δ EmissionVOC/ ΔT $Tg yr^{-1} K^{-1}$	33		234 \pm 7		81 \pm 2		150 \pm 2	124 \pm 76
Scaled mass/ ΔT $Tg K^{-1}$	0.017		0.50 \pm 0.02		0.127 \pm 0.0003		0.243 \pm 0.003	
$4xCO_2$ Δ mass/ ΔT $Tg K^{-1}$	0.135 \pm 0.004		0.644 \pm 0.018		0.022 \pm 0.001		0.510 \pm 0.018	0.33 \pm 0.26
Δ lifetime/ ΔT % K^{-1}	1.1 \pm 0.2		33 \pm 6		-4.2 \pm 0.2			
α emissions $W m^{-2} K^{-1}$	-0.003		-0.28 \pm 0.03		-0.089 \pm 0.006		-0.070 \pm 0.009	-0.088 \pm 0.077
α mass $W m^{-2} K^{-1}$	-0.025 \pm 0.01		-0.359 \pm 0.03		-0.015 \pm 0.001		-0.148 \pm 0.02	-0.113 \pm 0.102

Table 9. Radiative efficiencies by emission and mass from $2xVOC$. Changes in emission and mass from $4xCO_2$ experiment. “scaled” refers to scaling the $2xVOC$ relations between mass and emissions by the $4xCO_2$ changes in emissions. α values are calculated assuming ERF is proportional to emissions or mass. Multi-model mean values of α use the multi-model mean radiative efficiencies and sensitivities to climate, so are different to the average of the individual model α values. Uncertainties for each model are errors in the mean based on interannual variability. Uncertainties in the multi-model results are standard deviation across the models.

4.2 Gas-phase feedbacks

4.2.1 Biogenic VOCs

To estimate the stratospheric-temperature adjusted radiative forcing (SARF) from the ozone changes, and to remove the effect of aerosols we use the clear-sky aerosol-free ERF (ERF_{csaf}) (table 10). However, this neglects any cloud adjustments caused by the ozone, and any cloud masking of the direct ozone SARF. For GFDL-ESM4 and CESM2-WACCM the magnitude of the ozone forcing is smaller than that for aerosols leading to a net negative ERF from BVOCs. For UKESM1 the net ERF is positive due to a lower magnitude of aerosol forcing. The ozone contribution is also estimated assuming a radiative efficiency of 0.042 W/m^2 per Dobson Unit (Stevenson et al., 2013). This efficiency is strictly only applicable to



285 changes in tropospheric ozone but is also applied to the stratospheric ozone since these changes occur in the lower stratosphere just above the tropopause. The estimated ozone SARF (tropospheric + stratospheric) is within the range of the diagnosed ERF_{csaf} . CESM2-WACCM has the largest BVOC emissions and a decrease in tropospheric ozone column, although a strong increase in the stratospheric column. This is likely to be due to NO_x -limited chemistry near the surface and increased transport of reactive nitrogen (NO_y) away from the surface to the upper troposphere and lower stratosphere as peroxy-acetyl nitrate (PAN) and other organic nitrates. The overall feedback ranges from $0.004 \text{ W m}^{-2} \text{ K}^{-1}$ for UKESM1 which has the lowest ozone response to BVOC emissions, and the lowest BVOC increase with climate (due to CO_2 inhibition) to $0.028 \text{ W m}^{-2} \text{ K}^{-1}$ for CESM2-WACCM which has the strongest VOC response to climate.

290

	UKESM1		GFDL-ESM4		CESM2-WACCM		Multi-model	
$ERF_{csaf} 2xVOC$ W m^{-2}	0.09±0.03		0.13±0.04					
$ERF_{csaf}/\text{emission}$ $\text{W m}^2(\text{Tg yr}^{-1})^{-1}$	1.2±0.4E-4		2.8±0.8E-4					
	trop	strat	trop	strat	trop	strat		
Ozone/emission $\text{DU} (\text{Tg yr}^{-1})^{-1}$	0.0015	0.0021	0.0022	0.0031	-0.0003	0.0044		
Ozone SARF /emission $\text{W m}^2(\text{Tg yr}^{-1})^{-1}$	0.63±0.09 E-4	0.9±0.1 E-4	0.9±0.1 E-4	1.3±0.2 E-4	-0.10±0.01 E-4	1.8±0.3 E-4		
$4xCO_2$ $\text{Tg yr}^{-1} \text{ K}^{-1}$	32.5±0.8		81±2		150±2			
αERF_{csaf} $\text{W m}^{-2} \text{ K}^{-1}$	0.004±0.001		0.023±0.007					
$\alpha SARF_{O_3}$ $\text{W m}^{-2} \text{ K}^{-1}$	0.0021± 0.0003	0.0028± 0.0004	0.0076± 0.0011	0.011± 0.001	-0.0015± 0.0002	0.028± 0.004	0.003± 0.0040	0.014± 0.010

295 **Table 10. Radiative efficiencies (clear-sky aerosol-free ERF_{csaf}) for $2xVOC$ emissions. Tropospheric and stratospheric ozone column changes and their estimated radiative effects. Changes in emission from $4xCO_2$ experiment. α values are calculated assuming ERF_{csaf} or a SARF efficiency for ozone of $0.042 \text{ W m}^{-2} \text{ DU}^{-1}$. Uncertainties for each model are errors in the mean based on interannual variability, and assuming a 14% uncertainty in the ozone radiative efficiency. Uncertainties in the multi-model results are standard deviation across the models.**



BVOC emissions also affect the methane lifetime. Methane does not change in the AerChemMIP experimental setup, but the methane changes that would be expected if methane were allowed to evolve freely can be diagnosed from the change in methane lifetime. We diagnose this from changes in methane loss rate throughout the atmosphere (which includes stratospheric loss processes) and assume a loss to soils with a lifetime of 120 years (Ciais et al., 2013). All three models show similar sensitivities 0.030 to 0.047 % increase in methane lifetime per Tg yr⁻¹ of BVOC change due to decreases in OH in the mid-upper tropical free troposphere (not shown). From this the expected lifetime changes can be deduced from the change in BVOC emissions with temperature (table 11). These lifetime changes are converted to feedbacks using the radiative efficiency (including impacts on ozone and stratospheric water vapour) for methane lifetime changes in section 2.2 (0.015 W m⁻² %⁻¹). The feedbacks range from 0.012 to 0.081 W m⁻² K⁻¹ where the variability is mostly due to the different sensitivities of BVOCs to climate in the models. These are significantly stronger feedbacks than those due to ozone.

	UKESM1	GFDL-ESM4	CESM2-WACCM	Multi-model
$\tau_{\text{CH}_4}/\text{emission \% (Tg yr}^{-1}\text{)}^{-1}$	0.033	0.030	0.047	
$\tau_{\text{CH}_4}/\Delta T \% \text{ K}^{-1}$	1.1	2.4	7.1	
$\alpha \tau_{\text{CH}_4}$ W m ⁻² K ⁻¹	0.012±0.002	0.028±0.004	0.081±0.011	0.041±0.030

Table 11. Percentage change in methane lifetime for 2xVOC emissions. Estimated change in lifetime following changes in BVOC emission from 4xCO₂ experiment. α values are calculated assuming a radiative efficiency of 0.015 W m⁻² %⁻¹. Uncertainties for each model assume a 14% uncertainty in the methane radiative efficiency. Uncertainties in the multi-model results are standard deviation across the models.

4.2.2 Lightning NO_x

Lightning NO_x leads to ozone production, and changes in methane lifetime. In UKESM1 NO_x is known to increase the formation of new sulphate particles (O'Connor and et al., submitted) offsetting positive ozone forcing. To separate the ozone effect, we use ERF_{csaf} for UKESM1 as in section 4.2.1. The assumption of radiative efficiency of 0.042 W m⁻² DU⁻¹ seems to agree with the ERF for GFDL-ESM and CESM2-WACCM (table 12). For UKESM1 ERF_{csaf} is lower than expected from the ozone columns, suggesting that the clear-sky aerosol free component misses some of the ERF due to ozone.

Lightning NO_x increases in UKESM1 and CESM2-WACCM but decreases slightly in GFDL-ESM4 although they all use variations on the cloud-top height schemes (Price et al., 1997; Price and Rind, 1992). Hence the feedback is positive for UKESM1 and CESM2-WACCM (0.009 and 0.011 W m⁻² K⁻¹), based on the ozone changes, but slightly negative for GFDL-ESM4 (-0.001 W m⁻² K⁻¹).



	UKESM1		GFDL-ESM4		CESM2-WACCM		Multi-model	
ERF $2xNOX$ $W m^{-2}$	0.12±0.03		0.11±0.04		0.15±0.04			
ERF/emission $W m^2(Tg yr^{-1})^{-1}$	0.018±0.004		0.036±0.013		0.050±0.013			
	trop	strat	trop	strat	Trop	strat		
Ozone/emission $DU (Tg yr^{-1})^{-1}$	0.59	0.13	0.72	0.22	0.90	0.37		
Ozone SARF /emission $W m^2(Tg yr^{-1})^{-1}$	0.025± 0.003	0.0055± 0.0007	0.030± 0.004	0.009± 0.001	0.038± 0.005	0.015± 0.002		
$4xCO2$ $Tg yr^{-1} K^{-1}$	0.27±0.01		-0.029±0.008		0.208±0.006			
α ERF _{csaf} $W m^{-2} K^{-1}$	0.005±0.001		-0.0010±0.0005		0.010±0.003			
α SARF _{O3} $W m^{-2} K^{-1}$	0.007± 0.001	0.0015± 0.0002	-0.0009± 0.0003	0.000±0.001	0.008± 0.003	0.0032± 0.0005	0.005± 0.004	0.001± 0.001

325 **Table 12. Radiative efficiencies (clear-sky aerosol-free ERF_{csaf} for UKESM) for $2xNOX$ lightning NO_x emissions. Tropospheric and stratospheric ozone column changes and their estimated radiative effects. Changes in emission from $4xCO2$ experiment. α values are calculated assuming ERF_{csaf} or a SARF efficiency for ozone of $0.042 W m^{-2} DU^{-1}$. Uncertainties for each model are errors in the mean based on interannual variability, and assuming a 14% uncertainty in the ozone radiative efficiency. Uncertainties in the multi-model results are standard deviation across the models.**

330

As with BVOC emissions (above) the potential impacts of lightning on methane lifetime can be diagnosed. All models show (table 13) a decrease in methane lifetime with increased lightning NO_x emission from -2.3 to -4.8 % $(Tg yr^{-1})^{-1}$. The feedbacks are negative for UKESM1 and CESM2-WACCM (0.007 and $0.012 W m^{-2} K^{-1}$) and slightly positive for GFDL-ESM4 ($0.001 W m^{-2} K^{-1}$) and almost exactly cancel out the feedback due to the ozone column. The net (ozone + τ_{CH_4}) feedbacks for

335 UKESM1, GFDL-ESM4 and CESM2-WACCM are -0.002 , 0.000 , and $0.001 W m^{-2} K^{-1}$. For UKESM1 a feedback of $-0.006 W m^{-2} K^{-1}$ should be added to account for the increase in sulphate.



	UKESM1	GFDL-ESM4	CESM2-WACCM	Multi-model
τ_{CH_4} /emission % (Tg yr ⁻¹) ⁻¹	-2.3	-3.8	-4.8	
$\tau_{\text{CH}_4}/\Delta T$ % K ⁻¹	-0.6	0.1	1.0	
$\alpha \tau_{\text{CH}_4}$ W m ⁻² K ⁻¹	-0.007±0.001	0.0012±0.0004	-0.012±0.002	-0.006±0.005

340 **Table 13. Percentage change in methane lifetime for lightning NO_x emissions. Estimated change in lifetime following changes in NO_x emission from 4xCO₂ experiment. α values are calculated assuming a radiative efficiency of 0.015 W m⁻² %⁻¹. Uncertainties for each model assume a 14% uncertainty in the methane radiative efficiency. Uncertainties in the multi-model results are standard deviation across the models.**

4.2.3 Wetland emissions

Although the wetland emissions do not directly affect methane concentrations in the model, changes in emission can be converted to concentration changes (section 2.2). UKESM and WACCM models with interactive wetland emissions show
 345 strong responses to climate change, leading to a feedback of 0.16±0.03 W m⁻² K⁻¹.

	UKESM1	CESM2-WACCM	Multi-model
4xCO ₂ Tg yr ⁻¹ K ⁻¹	40	60	
α W m ⁻² K ⁻¹	0.13±0.02	0.19±0.03	0.16±0.03

350 **Table 14. Sensitivity of wetland emissions to 4xCO₂ in two models. Feedback parameter assuming pre-industrial conditions. Uncertainties for each model assume a 14% uncertainty in the methane radiative efficiency. Uncertainties in the multi-model results are standard deviation across the models.**

4.2.4 Temperature and humidity

As well as through changes in natural emissions, climate change can affect ozone burden and methane lifetime directly as the production and loss reactions are sensitive to temperature and water vapour. Here we add the expected changes in ozone and
 355 methane lifetime due to changes in BVOCs and lightning NO_x from sections 4.2.1 and 4.2.2 above and compare those to the changes diagnosed from the 4xCO₂ experiments (table 15). The residual is then the direct effect of climate. For CESM2-WACCM and GFDL-ESM4 most of the total increase in tropospheric ozone can be explained by the changes in natural emissions (particularly BVOC) suggesting that non-emission drivers of tropospheric ozone change (temperature, humidity,



transport from the stratosphere, dry deposition) balance to have little net effect. Increases in stratospheric ozone are much
360 larger than expected from the changes in natural emissions, suggesting that meteorological changes (principally cooling
stratospheric temperatures) are the main driver. The tropospheric ozone change attributable to climate can be used to determine
a feedback which is only significant for UKESM1 ($-0.023 \text{ W m}^{-2} \text{ K}^{-1}$). The stratospheric ozone changes cannot simply be
converted to an ERF, since unlike for the natural emission (where the ozone changes were close to the tropopause) the
tropospheric radiative efficiency cannot be applied.

365 In UKESM and GFDL-ESM4 the meteorological changes decrease methane lifetime by similar amounts (-4.5 and -4.6% K^{-1})
and hence have similar feedbacks (-0.078 and $-0.080 \text{ W m}^{-2} \text{ K}^{-1}$). In the case of GFDL-ESM4 this leads to an overall decrease
in lifetime rather than the increase expected from natural emission changes (principally BVOC). In WACCM the overall effect
of climate is to increase the methane lifetime, almost entirely due to the increased BVOC emissions with little effect of
370 meteorological drivers. This is surprising since there is no known mechanism whereby temperature and humidity increases
can increase the methane lifetime. This could be due to non-linearity whereby the effect of increased VOCs on methane lifetime
is larger than expected from scaling the $2\times\text{VOC}$ experiment.

Combining the results from ozone and methane lifetime changes leads to overall feedbacks from temperature of -0.101 , -0.082
and $+0.015 \text{ W m}^{-2} \text{ K}^{-1}$ for the three models.

375



	UKESM1		GFDL-ESM4		CESM2-WACCM		Multi-model
	trop	strat	Trop	strat	trop	strat	
LNO _x +BVOC Ozone (DU K ⁻¹)	0.210± 0.007	0.102± 0.002	0.160± 0.007	0.247± 0.006	0.151± 0.005	0.734± 0.008	
4xCO ₂ Ozone (DU K ⁻¹)	-0.33±0.02	1.28±0.10	0.18±0.02	3.46±0.06	0.162±0.003	2.82±0.04	
Ozone residual (DU K ⁻¹)	-0.54±0.02	1.18±0.10	0.02±0.02	3.22±0.06	0.011±0.006	2.09±0.05	
α Ozone residual W m ⁻² K ⁻¹	-0.023±0.003		0.001±0.001		0.000±0.000		-0.007±0.011
LNO _x +BVOC τ _{CH₄} % K ⁻¹	0.43±0.04		+2.55±0.07		+6.05±0.09		
4xCO ₂ τ _{CH₄} % K ⁻¹	-4.08±0.02		-2.05±0.06		+6.92±0.06		
τ _{CH₄} residual % K ⁻¹	-4.51±0.04		-4.60±0.08		+0.87±0.11		
alpha τ _{CH₄} residual W m ⁻² K ⁻¹	-0.078±0.011		-0.080±0.011		0.015±0.003		-0.048±0.045

Table 15. Comparison of expected changes in ozone column and methane lifetime with that diagnosed from 4xCO₂. Residual is given by the difference and is converted to a feedback using radiative efficiencies for tropospheric ozone and methane lifetime.

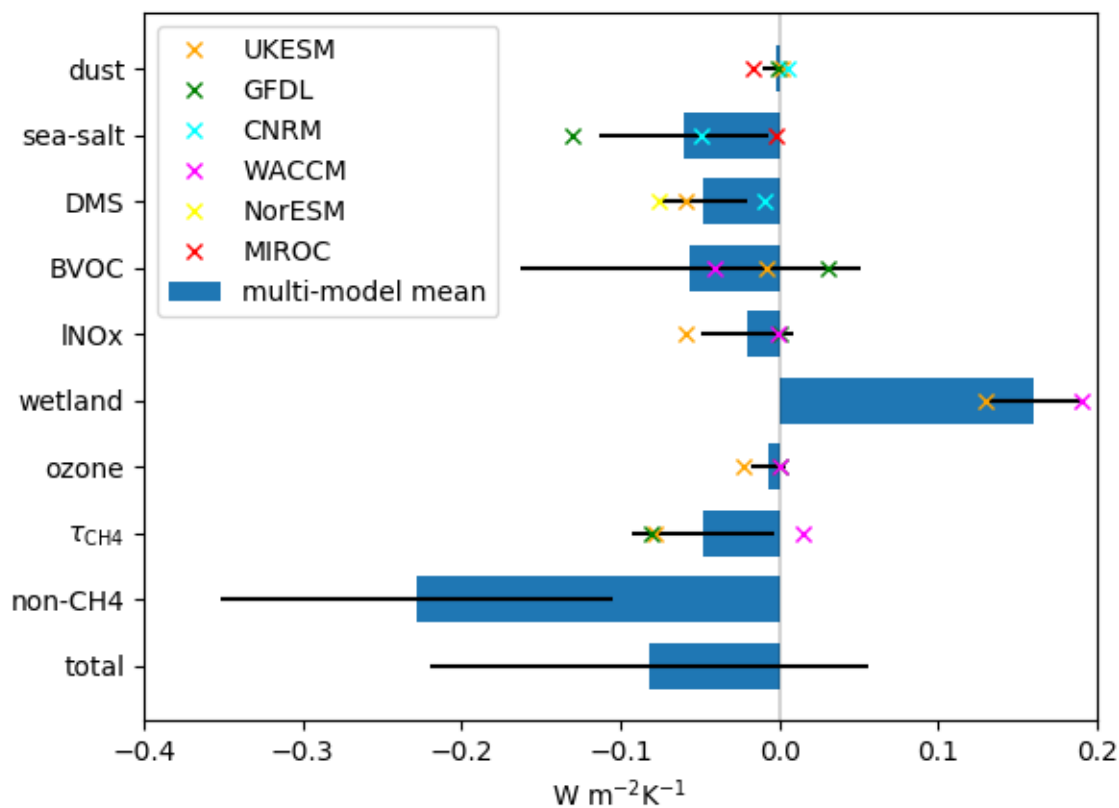
4.3 Overall feedback

380 The feedbacks are summarised in table 16. The largest individual feedbacks are due to the generation of aerosols by BVOCs
 (-0.113±0.102 W m² K¹) and the emission of methane from wetlands (0.16±0.03 W m² K¹). The overall uncertainty is
 dominated by the uncertainty in the aerosol response to BVOC emissions. Nearly all the feedbacks are negative, most because
 they come from an increase in aerosol with temperature. For BVOC emissions, the increase in aerosols outweighs the increases
 in ozone and methane. For lightning NO_x, the ozone and methane changes cancel. A warmer and more humid climate also
 385 leads to less ozone and methane.

The ESMs that use the *abrupt-4xCO₂* experiment to quantify the climate sensitivity do not allow methane to vary, so we also
 quantify the non-methane feedbacks that will be contributing to the diagnosed climate sensitivity in these models. This



feedback is significantly negative ($-0.228 \pm 0.123 \text{ W m}^{-2} \text{ K}^{-1}$) suggesting the climate sensitivity of ESMs might be expected to be lower than for their physical-only counterparts.



390

Figure 5. Feedback parameters of all the aerosol and chemical processes in table 16. Multi-model mean and individual models. Uncertainties are inter-model standard deviations. BVOC and INOx include aerosol, ozone and methane lifetime effects (points are only shown for models that include all effects). Non-CH₄ excludes methane lifetime effects and wetland feedback.



Process	Feedback parameter α ($\text{Wm}^{-2} \text{K}^{-1}$)
Dust (AOD)	-0.003 ± 0.008
Sea Salt (AOD)	-0.060 ± 0.053
DMS and sulphate lifetime	-0.048 ± 0.028
BVOC (Aerosol mass)	-0.113 ± 0.102
BVOC (ozone)	0.017 ± 0.011
BVOC (τ_{CH_4})	0.041 ± 0.030
INO _x (Aerosol)	-0.002 ± 0.003
INO _x (ozone)	0.006 ± 0.004
INO _x (τ_{CH_4})	-0.006 ± 0.005
Wetland	0.163 ± 0.032
Chemistry (ozone)	-0.007 ± 0.011
Chemistry (τ_{CH_4})	-0.048 ± 0.045
Total non-methane	-0.228 ± 0.123
Total	-0.082 ± 0.138

395 **Table 16. Feedback parameters of all the aerosol and chemical processes addressed in this study. Uncertainties are inter-model standard deviations.**

5. Discussion

5.1 Dust

400 Dust-aerosol feedback assessments are a relatively new area of research owing to the large uncertainties of climate models in simulating dust aerosols with changes in atmospheric composition. For instance, the spread in model estimates for dust aerosol changes in the 21st century is the largest among wildfires, biogenic SOA and DMS sulphate (Carslaw et al., 2010). Predictions for future dust emission range from an increase (Woodward et al., 2005) to a decrease (Mahowald and Luo, 2003). The modelled feedbacks in section 4.1.1 have a range of -0.016 to $+0.048 \text{ W m}^{-2} \text{ K}^{-1}$ compared to the theoretical model estimates of -0.04 to $+0.02 \text{ Wm}^{-2}\text{K}^{-1}$ by Kok et al. (2018).

405 The model ranges in dust forcing and feedbacks are not surprising in light of past studies that highlight model differences in dust-emitting winds and dust-aerosol parameterizations that contribute to the model diversity in the dust-aerosol loading, optical properties, and radiative effects (Ackerley et al., 2012; Evan et al., 2014; Huneeus et al., 2011; Shao et al., 2011; Zender et al., 2004). For instance, the parameterization of the planetary boundary layer plays an important role in determining the dust



loading, forcing, and regional feedbacks on winds (Alizadeh Choobari et al., 2012). Influencing factors for regional differences in the dust radiative effects are the surface albedo and aerosol size distribution (Kok et al., 2018; Xie et al., 2018), whereas
410 feedbacks on winds depend also on meteorological factors (Heinold et al., 2008). The substantial model differences in the dust emission response to $4\times CO_2$ paired with corresponding differences in mean 10m-wind speed in this study suggests that also the dust feedback parameter critically relies on accurately simulating atmospheric dynamics. Modelling atmospheric circulation has been identified as a grand challenge in climate research (Bony et al., 2015). Currently, we have no estimate which of the dust feedbacks shown are the most plausible, because convective dust storms are missing in such models, but this
415 dust storm type is believed to be important for North African dust emissions (Heinold et al., 2013). Moreover, natural aerosol-climate feedbacks are thought to depend on the anthropogenic aerosol burden and might therefore be both time-dependent and underestimated in the present-day polluted atmosphere (Spracklen and Rap, 2013). Taken together, we have a low confidence in the feedback estimates for dust aerosols to increases in atmospheric concentrations of greenhouse gases.

420

5.2 Sea Salt

The doubled sea salt ERF in section 4.1.2 is -0.35 to -2.28 $W\ m^{-2}$, higher end than found in the literature (-0.3 to -1.1 $W\ m^{-2}$ which is for direct forcing only (Yue and Liao, 2012)). The efficiency per AOD ranges from -20 to 39 $W\ m^{-2}$, again higher
425 than the literature for direct forcing (-18 to -24 $W\ m^{-2}$ (Heald et al., 2014; Yue and Liao, 2012)).

5.3 DMS

DMS is produced by marine biological activity in the ocean, and it is assumed to be the largest natural source of sulphur to the atmosphere. Up to now, there has been no comprehensive model effort to include all the important effects, and therefore the DMS emission strength change under climate change is still uncertain. The range here (-0.010 to -0.075 $W\ m^{-2}\ K^{-1}$ including
430 increases in sulphur lifetime) encompasses the -0.02 $W\ m^{-2}\ K^{-1}$ from AR5 (Ciais et al., 2013), based on results from only one model (HadGEM2-ES).

DMS production is closely linked to primary production. Modelling studies including ocean biogeochemistry have shown that under climate change, an increased stratification of the ocean at low and mid latitudes leads to a reduction in nutrients supply
435 into the surface ocean and thus a reduction in DMS emissions, whereas at high latitudes, retreat of sea-ice can lead to increased primary production and increase in DMS production (Kloster et al., 2007). Globally, most models which include ocean biogeochemistry show a slight increase in DMS production and emission to the atmosphere in a warming climate (Bopp et al., 2004; Gabric et al., 2004; Gunson et al., 2006; Vallina et al., 2007).



440 Some more recent studies have included the impact of ocean acidification on ocean DMS production (Schwinger et al., 2017;
Six et al., 2013). Both studies used a very similar description of the ocean biogeochemistry and extended it with an
observationally-based relation between ocean alkalinity and ocean DMS production. Assuming a medium sensitivity of the
DMS production on pH, Six et al. (2013) found a global DMS emission decrease by 18% in 2100 under the SRES A1B
scenario, and Schwinger et al. (2017) an emission reduction by 31% in 2200 under the RCP8.5 scenario. In addition recent
445 work has provided evidence for major pathways in the oxidation of DMS in the atmosphere which are not included in any of
these ESMs ((Berndt et al., 2019; Wu et al., 2015).

5.4 BVOC

When emissions of BVOCs are increased we see changes to organic aerosol concentration and (in some models) the
atmospheric concentrations or lifetime of O₃ and CH₄, with competing effects on climate. At the multi-model mean level, the
450 cooling associated with an increase in organic aerosol ($-0.113 \pm 0.102 \text{ W m}^{-2} \text{ K}^{-1}$) outweighs the warming associated with an
increase in O₃ ($0.017 \pm 0.011 \text{ W m}^{-2} \text{ K}^{-1}$) and an increase in CH₄ lifetime ($0.041 \pm 0.030 \text{ W m}^{-2} \text{ K}^{-1}$).

Using multi-annual simulations of global aerosol, Scott et al. (2018) diagnosed a feedback from biogenic secondary organic
aerosol of $-0.06 \text{ W m}^{-2} \text{ K}^{-1}$ globally, and $-0.03 \text{ W m}^{-2} \text{ K}^{-1}$ when considering only extra-tropical regions. This global feedback
value was composed of a direct aerosol radiative feedback of $-0.048 \text{ W m}^{-2} \text{ K}^{-1}$ and an indirect aerosol (i.e., cloud albedo)
455 feedback of $-0.013 \text{ W m}^{-2} \text{ K}^{-1}$. Using observations from eleven sites, Paasonen et al., (2013) estimated an indirect aerosol
feedback of $-0.01 \text{ W m}^{-2} \text{ K}^{-1}$ due to biogenic secondary organic aerosol. The ability of models to account for changes in
vegetation has a significant effect on the feedback. Sporre et al (2019) found interactive vegetation, enhanced BVOC emissions
by 63% greater relative to prescribed vegetation, producing more organic aerosol and an increase in (negative) aerosol forcing.
The level of compensation between increased aerosol forcing and increased ozone and methane lifetime is dependent on the
460 model (here positive feedback for GFDL, negative for UKESM1 and WACCM). Unger (2014) found a positive feedback in
NASA GISS ModelE2, whereas Scott et al. (2014) found a negative feedback in HadGEM2-ES.

5.5 Lightning

The ESMs used in CMIP6 all use a cloud-top height parameterisation of lightning. Such schemes have previously been found
to increase lightning production in warmer climates whereas more sophisticated schemes based on convective updraft mass
465 flux or ice flux show decreases in lightning with temperature. (Clark et al., 2017; Finney et al., 2016b, 2018). Two models
here (UKESM1 and WACCM) show increases in lightning emissions of 0.27 and 0.21 Tg(N) yr⁻¹ K⁻¹ which is slightly lower
than the results from the Atmospheric Chemistry and Climate Model Intercomparison (ACCMIP) of 0.44 Tg(N) yr⁻¹ K⁻¹
(Finney et al., 2016a).



5.6 Wetland methane

470 Wetland emissions are more strongly sensitive to CO₂ concentrations than to temperature or precipitation (Melton et al., 2013),
so the values presented here are more likely to be “adjustments” to the CO₂ rather than feedbacks, and hence could be
considered part of the CO₂ ERF. We find emission increases following quadrupled levels of CO₂ of 130-160%. This compares
with results from the Wetland CH₄ Inter-comparison of Models Project (WETCHIMP) of 20-160% following an increase in
CO₂ of a factor of 2.8 (Melton et al., 2013). The CMIP6 simulation specifications do not include free-running methane
475 concentrations therefore the effects of these increased wetland emissions will not be realised in any of the CMIP6 experiments.
Outside CMIP6, ESMs are starting to include free-running methane (Ocko et al., 2018), so for these it will be important to
understand the effects of changing CO₂ and meteorology on wetland emissions.

5.7 Temperature and humidity discussion

We find a decrease in methane lifetime of -4.5 to -4.6 % K⁻¹ in UKESM1 and GFDL-ESM4, but an increase of 0.9 % K⁻¹ in
480 WACCM. The first two models compare well with ACCMIP which found a sensitivity of 3.4±1.4% K⁻¹ (Naik et al., 2013;
Voulgarakis et al., 2013). The impact of climate (including natural emission changes) on tropospheric ozone varies from
negative in UKESM1 (-0.33 DU K⁻¹) to positive in GFDL-ESM4 and WACCM (0.18 and 0.16 DU K⁻¹). ACCMIP also found
a variation in sign amongst models -0.024±0.027 W m⁻² for a 1850-2000 change in climate (equivalent to -0.57±0.64 DU
485 either explicitly prescribed the cross-tropopause flux of ozone or imposed a climatology of ozone above the tropopause. The
three CMIP6 models here all treat the chemistry seamlessly across the troposphere and stratosphere so the impact of changes
in stratosphere-troposphere exchange (STE) of ozone on the tropospheric column is likely to be different to ACCMIP.
Changes in the stratospheric ozone column following a quadrupling of CO₂ are driven by cooling temperatures in the
stratosphere. This is likely to be due to temperature adjustments to the stratospheric CO₂ concentrations, and so part of the
490 ERF for CO₂ rather than a feedback (Smith, submitted). Feedbacks and adjustments cannot be distinguished with this
experimental setup.

6 Conclusions

Earth system models include more processes than physical-only climate models. These models will inherently include
additional climate feedbacks, and so have a different overall climate feedback (and climate sensitivity) to their physical
495 counterparts. In this study we consider six earth system models (CNRM-ESM2, UKESM1, MIROC6, NorESM2, GFDL-
ESM4, and CESM2-WACCM). Five of these (CNRM-ESM2, UKESM1, MIROC6, NorESM2 and GFDL-ESM4) participated
in the aerosol-related feedback experiments, and three (UKESM1, GFDL-ESM4, and CESM2-WACCM) in the chemistry-
related feedback experiments.



500 We focus in this study on the responses to an abrupt forcing of quadrupled CO₂ concentrations as that is the usual method to
diagnose climate feedbacks. By convention the feedbacks are quantified as a response to temperature (in W m⁻² K⁻¹), but they
may not necessarily be applicable to drivers of climate change other than CO₂ as some of the “feedbacks” may be instead
adjustments to CO₂ concentrations. It should also be noted that *abrupt-4xCO2* feedbacks are based on atmospheric conditions
representative of 1850s and thus may not be applicable to future responses starting from present day conditions.

505 Here we find that the dominant feedbacks are negative i.e. that they act to dampen the response to an imposed forcing. The
total feedback, excluding inferred changes in methane, is -0.228 ± 0.123 Wm⁻² K⁻¹. The increase in organic aerosols from
increase emission of volatile organic compounds (VOCs) from vegetation makes the largest contribution to both the magnitude
of the feedback and its uncertainty (-0.113 ± 0.102 Wm⁻² K⁻¹) with increases in sea salt and sulphate aerosol also contributing.
The increase in sulphate comes both from an increase in DMS emissions and a decrease in sulphate removal.

510 Contributions from increases in ozone production from biogenic VOCs and lightning NO_x are partially offset by decreased
tropospheric ozone lifetime in a warmer climate. Stratospheric ozone does substantially increase. Diagnoses of changes in
wetland emissions of methane indicate that if ESMs did allow methane to vary interactively the combined aerosol and chemical
feedbacks would be substantially less negative and consistent with zero.

Acknowledgements

515 GT, WC, RC-G, MM, FO’C, DO, MS, CES acknowledge funding received from the European Union’s Horizon 2020 research
and innovation programme under grant agreement No 641816 (CRESCENDO). MM acknowledges H2020 CONSTRAIN
under the grant agreement No 820829. CES acknowledges funding from the Natural Environment Research Council
(NE/S015396/1). FO.C, GF and JPM were supported by the Met Office Hadley Centre Climate Programme funded by BEIS
and Defra (GA01101).

520

Author Contributions

Manuscript preparation was by WC, GT, DO, RC-G, CES, SF and additional contributions from all co-authors. Model
simulations were provided by SB, GF, AG, , J-FL, MM, JM, PN, TT. Analysis was carried out by GT, WC, DO, SF, RC-G,
JW.



525 **Data Availability**

All data from the Earth system models used in this paper are available on the Earth System Grid Federation Website, and can be downloaded from there. <https://esgf-index1.ceda.ac.uk/search/cmip6-ceda/>

References

- 530 Ackerley, D., Joshi, M. M., Highwood, E. J., Ryder, C. L., Harrison, M. A. J., Walters, D. N., Milton, S. F. and Strachan, J.:
A comparison of two dust uplift schemes within the same general circulation model, *Adv. Meteorol.*,
doi:10.1155/2012/260515, 2012.
- Alizadeh Choobari, O., Zawar-Reza, P. and Sturman, A.: Feedback between windblown dust and planetary boundary-layer
characteristics: Sensitivity to boundary and surface layer parameterizations, *Atmos. Environ.*,
535 doi:10.1016/j.atmosenv.2012.07.038, 2012.
- Archibald, A., O'Connor, F., Archer-Nicholls, S., Chipperfield, M., Dalvi, M., Folberth, G., Dennison, F., Dhomse, S.,
Griffiths, P., Hardacre, C., Hewitt, A., Hill, R., Johnson, C., Keeble, J., Köhler, M., Morgenstern, O., Mulchay, J., Ordóñez,
C., Pope, R., Rumbold, S., Russo, M., Savage, N., Sellar, A., Stringer, M., Turnock, S., Wild, O. and Zeng, G.: Description
and evaluation of the UKCA stratosphere-troposphere chemistry scheme (StratTrop vn 1.0) implemented in UKESM1, *Geosci.*
540 *Model Dev. Discuss.*, doi:10.5194/gmd-2019-246, 2019.
- Arneth, A., Harrison, S. P., Zaehle, S., Tsigaridis, K., Menon, S., Bartlein, P. J., Feichter, J., Korhola, A., Kulmala, M.,
O'Donnell, D., Schurgers, G., Sorvari, S. and Vesala, T.: Terrestrial biogeochemical feedbacks in the climate system, *Nat.*
Geosci., 3(8), 525–532, doi:10.1038/ngeo905, 2010.
- Bates, T. S., Charlson, R. J. and Gammon, R. H.: Evidence for the climatic role of marine biogenic sulphur, *Nature*,
545 doi:10.1038/329319a0, 1987.
- Bellouin, N., Rae, J., Jones, A., Johnson, C., Haywood, J. and Boucher, O.: Aerosol forcing in the Climate Model
Intercomparison Project (CMIP5) simulations by HadGEM2-ES and the role of ammonium nitrate, *J. Geophys. Res. Atmos.*,
doi:10.1029/2011JD016074, 2011.
- Berndt, T., Scholz, W., Mentler, B., Fischer, L., Hoffmann, E. H., Tilgner, A., Hyttinen, N., Prisle, N. L., Hansel, A. and
550 Herrmann, H.: Fast Peroxy Radical Isomerization and OH Recycling in the Reaction of OH Radicals with Dimethyl Sulfide,
J. Phys. Chem. Lett., doi:10.1021/acs.jpcclett.9b02567, 2019.
- Bony, S., Stevens, B., Frierson, D. M. W., Jakob, C., Kageyama, M., Pincus, R., Shepherd, T. G., Sherwood, S. C., Siebesma,
A. P., Sobel, A. H., Watanabe, M. and Webb, M. J.: Clouds, circulation and climate sensitivity, *Nat. Geosci.*,
doi:10.1038/ngeo2398, 2015.
- 555 Bopp, L., Boucher, O., Aumont, O., Belviso, S., Dufresne, J. L., Pham, M. and Monfray, P.: Will marine dimethylsulfide
emissions amplify or alleviate global warming? A model study, in *Canadian Journal of Fisheries and Aquatic Sciences.*, 2004.



- Carslaw, K. S., Boucher, O., Spracklen, D. V., Mann, G. W., Rae, J. G. L., Woodward, S. and Kulmala, M.: Atmospheric Chemistry and Physics A review of natural aerosol interactions and feedbacks within the Earth system, *Atmos. Chem. Phys.*, 2010.
- 560 Ciais, P., Sabine, C., Bala, G., Bopp, L., Brovkin, V., Canadell, J., Chhabra, A., DeFries, R., Galloway, J., Heimann, M., Jones, C., Quéré, C. Le, Myneni, R. B., Piao, S. and Thornton, P.: Carbon and Other Biogeochemical Cycles, in *Climate Change 2013: The Physical Science Basis. Contribution of Working Group I to the Fifth Assessment Report of the Intergovernmental Panel on Climate Change*, edited by T. F. Stocker, D. Qin, G.-K. Plattner, M. Tignor, S. K. Allen, J. Boschung, A. Nauels, Y. Xia, V. Bex, and P. M. Midgley, pp. 465–570, Cambridge University Press, Cambridge, United Kingdom and New York, NY, USA., 2013.
- 565 Clark, S. K., Ward, D. S. and Mahowald, N. M.: Parameterization-based uncertainty in future lightning flash density, *Geophys. Res. Lett.*, doi:10.1002/2017GL073017, 2017.
- Collins, W., Lamarque, J. F., Schulz, M., Boucher, O., Eyring, V., Hegglin, M., Maycock, A., Myhre, G., Prather, M., Shindell, D. and Smith, S.: AerChemMIP: Quantifying the effects of chemistry and aerosols in CMIP6, *Geosci. Model Dev.*, 10(2), 570 585–607, doi:10.5194/gmd-10-585-2017, 2017.
- Collins, W. J., Bellouin, N., Doutriaux-Boucher, M., Gedney, N., Halloran, P., Hinton, T., Hughes, J., Jones, C. D., Joshi, M., Liddicoat, S., Martin, G., O’Connor, F., Rae, J., Senior, C., Sitch, S., Totterdell, I., Wiltshire, A. and Woodward, S.: Development and evaluation of an Earth-System model – HadGEM2, *Geosci. Model Dev.*, doi:10.5194/gmd-4-1051-2011, 2011.
- 575 Dentener, F., Kinne, S., Bond, T., Boucher, O., Cofala, J., Generoso, S., Ginoux, P., Gong, S., Hoelzemann, J. J., Ito, A., Marelli, L., Penner, J. E., Putaud, J. P., Textor, C., Schulz, M., Van Der Werf, G. R. and Wilson, J.: Emissions of primary aerosol and precursor gases in the years 2000 and 1750 prescribed data-sets for AeroCom, *Atmos. Chem. Phys.*, doi:10.5194/acp-6-4321-2006, 2006.
- Etminan, M., Myhre, G., Highwood, E. J. and Shine, K. P.: Radiative forcing of carbon dioxide, methane, and nitrous oxide: 580 A significant revision of the methane radiative forcing, *Geophys. Res. Lett.*, doi:10.1002/2016GL071930, 2016.
- Evan, A. T., Flamant, C., Fiedler, S. and Doherty, O.: An analysis of aeolian dust in climate models, *Geophys. Res. Lett.*, doi:10.1002/2014GL060545, 2014.
- Eyring, V., Bony, S., Meehl, G. A., Senior, C. A., Stevens, B., Stouffer, R. J. and Taylor, K. E.: Overview of the Coupled Model Intercomparison Project Phase 6 (CMIP6) experimental design and organization, *Geosci. Model Dev.*, 585 doi:10.5194/gmd-9-1937-2016, 2016.
- Fiedler, S., Knippertz, P., Woodward, S., Martin, G. M., Bellouin, N., Ross, A. N., Heinold, B., Schepanski, K., Birch, C. E. and Tegen, I.: A process-based evaluation of dust-emitting winds in the CMIP5 simulation of HadGEM2-ES, *Clim. Dyn.*, doi:10.1007/s00382-015-2635-9, 2016.
- Finney, D. L., Doherty, R. M., Wild, O., Young, P. J. and Butler, A.: Response of lightning NO_x emissions and ozone



- 590 production to climate change: Insights from the Atmospheric Chemistry and Climate Model Intercomparison Project, *Geophys. Res. Lett.*, doi:10.1002/2016GL068825, 2016a.
- Finney, D. L., Doherty, R. M., Wild, O. and Abraham, N. L.: The impact of lightning on tropospheric ozone chemistry using a new global lightning parametrisation, *Atmos. Chem. Phys.*, doi:10.5194/acp-16-7507-2016, 2016b.
- 595 Finney, D. L., Doherty, R. M., Wild, O., Stevenson, D. S., MacKenzie, I. A. and Blyth, A. M.: A projected decrease in lightning under climate change, *Nat. Clim. Chang.*, doi:10.1038/s41558-018-0072-6, 2018.
- Fiore, A. M., Dentener, F. J., Wild, O., Cuvelier, C., Schultz, M. G., Hess, P., Textor, C., Schulz, M., Doherty, R. M., Horowitz, L. W., MacKenzie, I. A., Sanderson, M. G., Shindell, D. T., Stevenson, D. S., Szopa, S., Van Dingenen, R., Zeng, G., Atherton, C., Bergmann, D., Bey, I., Carmichael, G., Collins, W. J., Duncan, B. N., Faluvegi, G., Folberth, G., Gauss, M., Gong, S., Hauglustaine, D., Holloway, T., Isaksen, I. S. A., Jacob, D. J., Jonson, J. E., Kaminski, J. W., Keating, T. J., Lupu, A., Manner, E., Montanaro, V., Park, R. J., Pitari, G., Pringle, K. J., Pyle, J. A., Schroeder, S., Vivanco, M. G., Wind, P., Wojcik, G., Wu, S. and Zuber, A.: Multimodel estimates of intercontinental source-receptor relationships for ozone pollution, *J. Geophys. Res. Atmos.*, 114(4), doi:10.1029/2008JD010816, 2009.
- 600 Gabric, A. J., Simó, R., Cropp, R. A., Hirst, A. C. and Dachs, J.: Modeling estimates of the global emission of dimethylsulfide under enhanced greenhouse conditions, *Global Biogeochem. Cycles*, doi:10.1029/2003GB002183, 2004.
- 605 Gantt, B., Johnson, M. S., Meskhidze, N., Sciare, J., Ovadnevaite, J., Ceburnis, D. and O'Dowd, C. D.: Model evaluation of marine primary organic aerosol emission schemes, *Atmos. Chem. Phys.*, doi:10.5194/acp-12-8553-2012, 2012.
- Gettelman, A., Mills, M. J., Kinnison, D. E., Garcia, R. R., Smith, A. K., Marsh, D. R., Tilmes, S., Vitt, F., Bardeen, C. G., McInerney, J., Liu, H. -L., Solomon, S. C., Polvani, L. M., Emmons, L. K., Lamarque, J. -F., Richter, J. H., Glanville, A. S., Bacmeister, J. T., Phillips, A. S., Neale, R. B., Simpson, I. R., DuVivier, A. K., Hodzic, A. and Randel, W. J.: The Whole Atmosphere Community Climate Model Version 6 (WACCM6), *J. Geophys. Res. Atmos.*, doi:10.1029/2019jd030943, 2019.
- 610 Ghan, S. J.: Technical note: Estimating aerosol effects on cloud radiative forcing, *Atmos. Chem. Phys.*, doi:10.5194/acp-13-9971-2013, 2013.
- Gong, S. L.: A parameterization of sea-salt aerosol source function for sub- and super-micron particles, *Global Biogeochem. Cycles*, doi:10.1029/2003gb002079, 2003.
- 615 Gregory, J. M., Ingram, W. J., Palmer, M. A., Jones, G. S., Stott, P. A., Thorpe, R. B., Lowe, J. A., Johns, T. C. and Williams, K. D.: A new method for diagnosing radiative forcing and climate sensitivity, *Geophys. Res. Lett.*, 31(3), L03205, doi:10.1029/2003GL018747, 2004.
- Gregory, J. M., Jones, C. D., Cadule, P. and Friedlingstein, P.: Quantifying carbon cycle feedbacks, *J. Clim.*, doi:10.1175/2009JCLI2949.1, 2009.
- 620 Grythe, H., Ström, J., Krejci, R., Quinn, P. and Stohl, A.: A review of sea-spray aerosol source functions using a large global set of sea salt aerosol concentration measurements, *Atmos. Chem. Phys.*, doi:10.5194/acp-14-1277-2014, 2014.
- Guenther, A.: A global model of natural volatile organic compound emissions, *J. Geophys. Res.*, doi:10.1029/94JD02950,



- 1995.
- Guenther, A. B., Jiang, X., Heald, C. L., Sakulyanontvittaya, T., Duhl, T., Emmons, L. K. and Wang, X.: The model of emissions of gases and aerosols from nature version 2.1 (MEGAN2.1): An extended and updated framework for modeling biogenic emissions, *Geosci. Model Dev.*, doi:10.5194/gmd-5-1471-2012, 2012.
- Gunson, J. R., Spall, S. A., Anderson, T. R., Jones, A., Totterdell, I. J. and Woodage, M. J.: Climate sensitivity to ocean dimethylsulphide emissions, *Geophys. Res. Lett.*, doi:10.1029/2005GL024982, 2006.
- Heald, C. L., Ridley, D. A., Kroll, J. H., Barrett, S. R. H., Cady-Pereira, K. E., Alvarado, M. J. and Holmes, C. D.: Contrasting the direct radiative effect and direct radiative forcing of aerosols, *Atmos. Chem. Phys.*, doi:10.5194/acp-14-5513-2014, 2014.
- Heinold, B., Tegen, I., Schepanski, K. and Hellmuth, O.: Dust radiative feedback on Saharan boundary layer dynamics and dust mobilization, *Geophys. Res. Lett.*, doi:10.1029/2008GL035319, 2008.
- Heinold, B., Knippertz, P., Marsham, J. H., Fiedler, S., Dixon, N. S., Schepanski, K., Laurent, B. and Tegen, I.: The role of deep convection and nocturnal low-level jets for dust emission in summertime West Africa: Estimates from convection-permitting simulations, *J. Geophys. Res. Atmos.*, doi:10.1002/jgrd.50402, 2013.
- Heinze, C., Eyring, V., Friedlingstein, P., Jones, C., Balkanski, Y., Collins, W., Fichet, T., Gao, S., Hall, A., Ivanova, D., Knorr, W., Knutti, R., Löw, A., Ponater, M., Schultz, M., Schulz, M., Siebesma, P., Teixeira, J., Tselioudis, G. and Vancoppenolle, M.: ESD Reviews: Climate feedbacks in the Earth system and prospects for their evaluation, *Earth Syst. Dyn.*, doi:10.5194/esd-10-379-2019, 2019.
- Huneus, N., Schulz, M., Balkanski, Y., Griesfeller, J., Prospero, J., Kinne, S., Bauer, S., Boucher, O., Chin, M., Dentener, F., Diehl, T., Easter, R., Fillmore, D., Ghan, S., Ginoux, P., Grini, A., Horowitz, L., Koch, D., Krol, M. C., Landing, W., Liu, X., Mahowald, N., Miller, R., Morcrette, J. J., Myhre, G., Penner, J., Perlwitz, J., Stier, P., Takemura, T. and Zender, C. S.: Global dust model intercomparison in AeroCom phase i, *Atmos. Chem. Phys.*, doi:10.5194/acp-11-7781-2011, 2011.
- Jaeglé, L., Quinn, P. K., Bates, T. S., Alexander, B. and Lin, J. T.: Global distribution of sea salt aerosols: New constraints from in situ and remote sensing observations, *Atmos. Chem. Phys.*, doi:10.5194/acp-11-3137-2011, 2011.
- Kettle, A. J., Andreae, M. O., Amouroux, D., Andreae, T. W., Bates, T. S., Berresheim, H., Bingemer, H., Boniforti, R., Curran, M. A. J., DiTullio, G. R., Helas, G., Jones, G. B., Keller, M. D., Kiene, R. P., Leek, C., Lévassieur, M., Malin, G., Maspero, M., Matrai, P., McTaggart, A. R., Mihalopoulos, N., Nguyen, B. C., Novo, A., Putaud, J. P., Rapsomanikis, S., Roberts, G., Schebeske, G., Sharma, S., Simó, R., Staubes, R., Turner, S. and Uher, G.: A global database of sea surface dimethylsulfide (DMS) measurements and a procedure to predict sea surface DMS as a function of latitude, longitude, and month, *Global Biogeochem. Cycles*, doi:10.1029/1999GB900004, 1999.
- Kirkevåg, A., Grini, A., Oliví, D., Seland, Ø., Alterskjær, K., Hummel, M., Karset, I. H. H., Lewinschal, A., Liu, X., Makkonen, R., Bethke, I., Griesfeller, J., Schulz, M. and Iversen, T.: A production-tagged aerosol module for earth system models, *OsloAero5.3-extensions and updates for CAM5.3-Oslo*, *Geosci. Model Dev.*, doi:10.5194/gmd-11-3945-2018, 2018.
- Kloster, S., Six, K. D., Feichter, J., Maier-Reimer, E., Roeckner, E., Wetzell, P., Stier, P. and Esch, M.: Response of



- dimethylsulfide (DMS) in the ocean and atmosphere to global warming, *J. Geophys. Res. Biogeosciences*, doi:10.1029/2006JG000224, 2007.
- Kok, J. F., Ward, D. S., Mahowald, N. M. and Evan, A. T.: Global and regional importance of the direct dust-climate feedback, *Nat. Commun.*, doi:10.1038/s41467-017-02620-y, 2018.
- 660 Mahowald, N. M. and Luo, C.: A less dusty future?, *Geophys. Res. Lett.*, doi:10.1029/2003GL017880, 2003.
- Melton, J. R., Wania, R., Hodson, E. L., Poulter, B., Ringeval, B., Spahni, R., Bohn, T., Avis, C. A., Beerling, D. J., Chen, G., Eliseev, A. V., Denisov, S. N., Hopcroft, P. O., Lettenmaier, D. P., Riley, W. J., Singarayer, J. S., Subin, Z. M., Tian, H., Zürcher, S., Brovkin, V., Van Bodegom, P. M., Kleinen, T., Yu, Z. C. and Kaplan, J. O.: Present state of global wetland extent and wetland methane modelling: Conclusions from a model inter-comparison project (WETCHIMP), *Biogeosciences*, doi:10.5194/bg-10-753-2013, 2013.
- 665 Michou, M., Nabat, P. and Saint-Martin, D.: Development and basic evaluation of a prognostic aerosol scheme in the CNRM Climate Model, *Geosci. Model Dev. Discuss.*, doi:10.5194/gmdd-7-6263-2014, 2014.
- Monahan, E. C.: *The Ocean as a Source for Atmospheric Particles, in The Role of Air-Sea Exchange in Geochemical Cycling.*, 1986.
- 670 Monahan, E. C. and Muircheartaigh, I. O.: Optimal power-law description of oceanic whitecap coverage dependence on wind speed., *J. PHYS. Ocean.*, doi:10.1175/1520-0485(1980)010<2094:opldoo>2.0.co;2, 1980.
- Mulcahy, J. P., Johnson, C., Jones, C. G., Povey, A. C., Scott, C. E., Sellar, A., Turnock, S. T., Woodhouse, M. T., Abraham, N. L., Andrews, M. B., Bellouin, N., Browse, J., Carslaw, K. S., Dalvi, M., Folberth, G. A., Glover, M., Grosvenor, D., Hardacre, C., Hill, R., Johnson, B., Jones, A., Kipling, Z., Mann, G., Mollard, J., Connor, O. F. M., Palmieri, J., Reddington, C., Rumbold, S. T., Richardson, M., Schutgens, N. A. J., Stier, P., Stringer, M., Tang, Y., Walton, J., Woodward, S. and Yool, A.: Description and evaluation of aerosol in UKESM1 and HadGEM3-GC3.1 CMIP6 historical simulations, *Geosci. Model Dev. Discuss.*, 2019.
- 675 Myhre, G., Shindell, D., Bréon, F.-M., Collins, W., Fuglestedt, J., Huang, J., Koch, D., Lamarque, J.-F., Lee, D., Mendoza, B., Nakajima, T., Robock, A., Stephens, G., Takemura, T. and Zhang, H.: Anthropogenic and Natural Radiative Forcing, in *Climate Change 2013: The Physical Science Basis. Contribution of Working Group I to the Fifth Assessment Report of the Intergovernmental Panel on Climate Change*, edited by T. F. Stocker, D. Qin, G.-K. Plattner, M. Tignor, S. K. Allen, J. Boschung, A. Nauels, Y. Xia, V. Bex, and P. M. Midgley, pp. 659–740, Cambridge University Press, Cambridge, United Kingdom and New York, NY, USA., 2013.
- 680 Naik, V., Voulgarakis, A., Fiore, A. M., Horowitz, L. W., Lamarque, J.-F., Lin, M., Prather, M. J., Young, P. J., Bergmann, D., Cameron-Smith, P. J., Cionni, I., Collins, W. J., Dalsøren, S. B., Doherty, R., Eyring, V., Faluvegi, G., Folberth, G. A., Josse, B., Lee, Y. H., MacKenzie, I. A., Nagashima, T., Van Noije, T. P. C., Plummer, D. A., Righi, M., Rumbold, S. T., Skeie, R., Shindell, D. T., Stevenson, D. S., Strode, S., Sudo, K., Szopa, S. and Zeng, G.: Preindustrial to present-day changes in tropospheric hydroxyl radical and methane lifetime from the Atmospheric Chemistry and Climate Model Intercomparison



- Project (ACCMIP), *Atmos. Chem. Phys.*, 13(10), doi:10.5194/acp-13-5277-2013, 2013.
- 690 Nightingale, P. D., Malin, G., Law, C. S., Watson, A. J., Liss, P. S., Liddicoat, M. I., Boutin, J. and Upstill-Goddard, R. C.: In situ evaluation of air-sea gas exchange parameterizations using novel conservative and volatile tracers, *Global Biogeochem. Cycles*, doi:10.1029/1999GB900091, 2000.
- O'Connor, F. M. and et al.: Pre-industrial to present-day anthropogenic effective radiative forcings (ERFs) from UKESM1, *Acpd*, in *progres*(1), 2019.
- 695 O'Connor, F. M., Boucher, O., Gedney, N., Jones, C. D., Folberth, G. A., Coppel, R., Friedlingstein, P., Collins, W. J., Chappellaz, J., Ridley, J. and Johnson, C. E.: Possible role of wetlands, permafrost, and methane hydrates in the methane cycle under future climate change: A review, *Rev. Geophys.*, doi:10.1029/2010RG000326, 2010.
- O'Dowd, C. D., Langmann, B., Varghese, S., Scannell, C., Ceburnis, D. and Facchini, M. C.: A combined organic-inorganic sea-spray source function, *Geophys. Res. Lett.*, doi:10.1029/2007GL030331, 2008.
- 700 Ocko, I. B., Naik, V. and Paynter, D.: Rapid and reliable assessment of methane impacts on climate, *Atmos. Chem. Phys.*, doi:10.5194/acp-18-15555-2018, 2018.
- Paasonen, P., Asmi, A., Petäjä, T., Kajos, M. K., Äijälä, M., Junninen, H., Holst, T., Abbatt, J. P. D., Arneth, A., Birmili, W., Van Der Gon, H. D., Hamed, A., Hoffer, A., Laakso, L., Laaksonen, A., Richard Leaitch, W., Plass-Dülmer, C., Pryor, S. C., Räisänen, P., Swietlicki, E., Wiedensohler, A., Worsnop, D. R., Kerminen, V. M. and Kulmala, M.: Warming-induced increase
705 in aerosol number concentration likely to moderate climate change, *Nat. Geosci.*, doi:10.1038/ngeo1800, 2013.
- Pacifico, F., Harrison, S. P., Jones, C. D., Arneth, A., Sitch, S., Weedon, G. P., Barkley, M. P., Palmer, P. I., Serça, D., Potosnak, M., Fu, T. M., Goldstein, A., Bai, J. and Schurgers, G.: Evaluation of a photosynthesis-based biogenic isoprene emission scheme in JULES and simulation of isoprene emissions under present-day climate conditions, *Atmos. Chem. Phys.*, doi:10.5194/acp-11-4371-2011, 2011.
- 710 Pacifico, F., Folberth, G. A., Jones, C. D., Harrison, S. P. and Collins, W. J.: Sensitivity of biogenic isoprene emissions to past, present, and future environmental conditions and implications for atmospheric chemistry, *J. Geophys. Res. Atmos.*, 117(22), doi:10.1029/2012JD018276, 2012.
- Price, C. and Rind, D.: A simple lightning parameterization for calculating global lightning distributions, *J. Geophys. Res.*, doi:10.1029/92JD00719, 1992.
- 715 Price, C., Penner, J. and Prather, M.: NO_x from lightning 1. Global distribution based on lightning physics, *J. Geophys. Res. Atmos.*, doi:10.1029/96jd03504, 1997.
- Raes, F., Liao, H., Chen, W. T. and Seinfeld, J. H.: Atmospheric chemistry-climate feedbacks, *J. Geophys. Res. Atmos.*, doi:10.1029/2009JD013300, 2010.
- Salter, M. E., Zieger, P., Acosta Navarro, J. C., Grythe, H., Kirkevåg, A., Rosati, B., Riipinen, I. and Nilsson, E. D.: An
720 empirically derived inorganic sea spray source function incorporating sea surface temperature, *Atmos. Chem. Phys.*, doi:10.5194/acp-15-11047-2015, 2015.



- Schwinger, J., Tjiputra, J., Goris, N., Six, K. D., Kirkevåg, A., Seland, Ø., Heinze, C. and Ilyina, T.: Amplification of global warming through pH dependence of DMS production simulated with a fully coupled Earth system model, *Biogeosciences*, doi:10.5194/bg-14-3633-2017, 2017.
- 725 Scott, C. E., Rap, A., Spracklen, D. V., Forster, P. M., Carslaw, K. S., Mann, G. W., Pringle, K. J., Kivekäs, N., Kulmala, M., Lihavainen, H. and Tunved, P.: The direct and indirect radiative effects of biogenic secondary organic aerosol, *Atmos. Chem. Phys.*, doi:10.5194/acp-14-447-2014, 2014.
- Scott, C. E., Arnold, S. R., Monks, S. A., Asmi, A., Paasonen, P. and Spracklen, D. V.: Substantial large-scale feedbacks between natural aerosols and climate, *Nat. Geosci.*, doi:10.1038/s41561-017-0020-5, 2018.
- 730 Séférian, R., Nabat, P., Michou, M., Saint-Martin, D., Voldoire, A., Colin, J., Decharme, B., Delire, C., Berthet, S., Chevallier, M., Sénési, S., Franchisteguy, L., Vial, J., Mallet, M., Joetzjer, E., Geoffroy, O., Guérémy, J. -F., Moine, M. -P., Msadek, R., Ribes, A., Rocher, M., Roehrig, R., Salas-y-Méla, D., Sanchez, E., Terray, L., Valcke, S., Waldman, R., Aumont, O., Bopp, L., Deshayes, J., Éthé, C. and Madec, G.: Evaluation of CNRM Earth-System model, CNRM-ESM 2-1: role of Earth system processes in present-day and future climate, *J. Adv. Model. Earth Syst.*, doi:10.1029/2019MS001791, 2019.
- 735 Sellar, A. A., Jones, C. G., Mulcahy, J., Tang, Y., Yool, A., Wiltshire, A., O'Connor, F. M., Stringer, M., Hill, R., Palmieri, J., Woodward, S., Mora, L., Kuhlbrodt, T., Rumbold, S., Kelley, D. I., Ellis, R., Johnson, C. E., Walton, J., Abraham, N. L., Andrews, M. B., Andrews, T., Archibald, A. T., Berthou, S., Burke, E., Blockley, E., Carslaw, K., Dalvi, M., Edwards, J., Folberth, G. A., Gedney, N., Griffiths, P. T., Harper, A. B., Hendry, M. A., Hewitt, A. J., Johnson, B., Jones, A., Jones, C. D., Keeble, J., Liddicoat, S., Morgenstern, O., Parker, R. J., Predoi, V., Robertson, E., Siahann, A., Smith, R. S., Swaminathan, R., Woodhouse, M. T., Zeng, G. and Zerroukat, M.: UKESM1: Description and evaluation of the UK Earth System Model, *J. Adv. Model. Earth Syst.*, doi:10.1029/2019ms001739, 2019.
- Shao, Y., Wyrwoll, K. H., Chappell, A., Huang, J., Lin, Z., McTainsh, G. H., Mikami, M., Tanaka, T. Y., Wang, X. and Yoon, S.: Dust cycle: An emerging core theme in Earth system science, *Aeolian Res.*, doi:10.1016/j.aeolia.2011.02.001, 2011.
- Six, K. D., Kloster, S., Ilyina, T., Archer, S. D., Zhang, K. and Maier-Reimer, E.: Global warming amplified by reduced sulphur fluxes as a result of ocean acidification, *Nat. Clim. Chang.*, doi:10.1038/nclimate1981, 2013.
- 745 Smith, C. J.: Effective radiative forcing and rapid adjustments in CMIP6 models, *Atmos. Chem. Phys.*, submitted..
- Sporre, M. K., Blichner, S. M., Karset, I. H. H., Makkonen, R. and Berntsen, T. K.: BVOC-aerosol-climate feedbacks investigated using NorESM, *Atmos. Chem. Phys.*, doi:10.5194/acp-19-4763-2019, 2019.
- Spracklen, D. V. and Rap, A.: Natural aerosol-climate feedbacks suppressed by anthropogenic aerosol, *Geophys. Res. Lett.*, doi:10.1002/2013GL057966, 2013.
- 750 Stevenson, D. S., Young, P. J., Naik, V., Lamarque, J.-F., Shindell, D. T., Voulgarakis, A., Skeie, R. B., Dalsoren, S. B., Myhre, G., Berntsen, T. K., Folberth, G. A., Rumbold, S. T., Collins, W. J., MacKenzie, I. A., Doherty, R. M., Zeng, G., Van Noije, T. P. C., Strunk, A., Bergmann, D., Cameron-Smith, P., Plummer, D. A., Strode, S. A., Horowitz, L., Lee, Y. H., Szopa, S., Sudo, K., Nagashima, T., Josse, B., Cionni, I., Righi, M., Eyring, V., Conley, A., Bowman, K. W., Wild, O. and Archibald,



- 755 A.: Tropospheric ozone changes, radiative forcing and attribution to emissions in the Atmospheric Chemistry and Climate Model Intercomparison Project (ACCMIP), *Atmos. Chem. Phys.*, 13(6), doi:10.5194/acp-13-3063-2013, 2013.
- Tatebe, H., Ogura, T., Nitta, T., Komuro, Y., Ogochi, K., Takemura, T., Sudo, K., Sekiguchi, M., Abe, M., Saito, F., Chikira, M., Watanabe, S., Mori, M., Hirota, N., Kawatani, Y., Mochizuki, T., Yoshimura, K., Takata, K., O’Ishi, R., Yamazaki, D., Suzuki, T., Kurogi, M., Kataoka, T., Watanabe, M. and Kimoto, M.: Description and basic evaluation of simulated mean state, internal variability, and climate sensitivity in MIROC6, *Geosci. Model Dev.*, doi:10.5194/gmd-12-2727-2019, 2019.
- 760 Thornhill, G., Collins, W., Connor, F. O., Smith, C., Kramer, R., Forster, P., Checa-garcia, R. and Schulz, M.: Effective Radiative forcing from emissions of reactive gases and aerosols - a multi-model comparison, *Atmos. Chem. Phys.*, n.d.
- Unger, N.: On the role of plant volatiles in anthropogenic global climate change, *Geophys. Res. Lett.*, doi:10.1002/2014GL061616, 2014.
- 765 Vallina, S. M., Simó, R. and Manizza, M.: Weak response of oceanic dimethylsulfide to upper mixing shoaling induced by global warming, *Proc. Natl. Acad. Sci. U. S. A.*, doi:10.1073/pnas.0700843104, 2007.
- Voulgarakis, A., Naik, V., Lamarque, J.-F., Shindell, D. T., Young, P. J., Prather, M. J., Wild, O., Field, R. D., Bergmann, D., Cameron-Smith, P., Cionni, I., Collins, W. J., Dalsøren, S. B., Doherty, R. M., Eyring, V., Faluvegi, G., Folberth, G. A., Horowitz, L. W., Josse, B., MacKenzie, I. A., Nagashima, T., Plummer, D. A., Righi, M., Rumbold, S. T., Stevenson, D. S., Strode, S. A., Sudo, K., Szopa, S. and Zeng, G.: Analysis of present day and future OH and methane lifetime in the ACCMIP simulations, *Atmos. Chem. Phys.*, 13(5), doi:10.5194/acp-13-2563-2013, 2013.
- 770 Woodward, S.: Modeling the atmospheric life cycle and radiative impact of mineral dust in the Hadley Centre climate model, *J. Geophys. Res. Atmos.*, doi:10.1029/2000JD900795, 2001.
- Woodward, S., Roberts, D. L. and Betts, R. A.: A simulation of the effect of climate change-induced desertification on mineral dust aerosol, *Geophys. Res. Lett.*, doi:10.1029/2005GL023482, 2005.
- 775 Wu, R., Wang, S. and Wang, L.: New mechanism for the atmospheric oxidation of dimethyl sulfide. The importance of intramolecular hydrogen shift in a CH₃SCH₂OO radical, *J. Phys. Chem. A*, doi:10.1021/jp511616j, 2015.
- Xie, X., Liu, X., Che, H., Xie, X., Wang, H., Li, J., Shi, Z. and Liu, Y.: Modeling East Asian Dust and Its Radiative Feedbacks in CAM4-BAM, *J. Geophys. Res. Atmos.*, doi:10.1002/2017JD027343, 2018.
- 780 Yue, X. and Liao, H.: Climatic responses to the shortwave and longwave direct radiative effects of sea salt aerosol in present day and the last glacial maximum, *Clim. Dyn.*, doi:10.1007/s00382-012-1312-5, 2012.
- Zender, C. S., Bian, H. and Newman, D.: Mineral Dust Entrainment and Deposition (DEAD) model: Description and 1990s dust climatology, *J. Geophys. Res. D Atmos.*, doi:10.1029/2002jd002775, 2003.
- Zender, C. S., Miller, R. L. and Tegen, I.: Quantifying mineral dust mass budgets: Terminology, constraints, and current estimates, *Eos (Washington. DC)*, doi:10.1029/2004EO480002, 2004.
- 785